

Link from “movie night”
worldwidetelescope.org



Astronomy as It

Alyssa A. Goodman

Professor of Astronomy
& Founding Director of the
Initiative in Innovative Computing,
Harvard University

Scholar-in-Residence,
WGBH Boston



Science + Technology

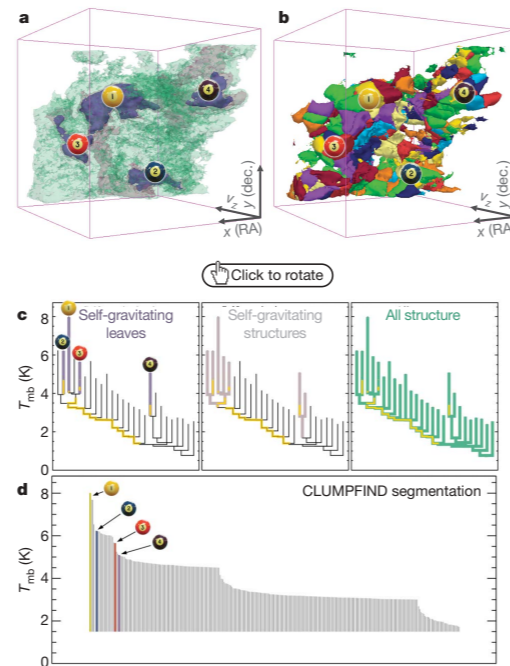


Figure 2 | Comparison of the 'dendrogram' and 'CLUMPFIND' feature-identification algorithms as applied to ^{13}CO emission from the L1448 region of Perseus. **a**, 3D visualization of the surfaces indicated by colours in the dendrogram shown in **c**. Purple illustrates the smallest scale self-gravitating structures in the region corresponding to the leaves of the dendrogram; pink shows the smallest surfaces that contain distinct self-gravitating leaves within them; and green corresponds to the surface in the data cube containing all the significant emission. Dendrogram branches corresponding to self-gravitating objects have been highlighted in yellow over the range of T_{mb} (main-beam temperature) test-level values for which the virial parameter is less than 2. The x - y locations of the four 'self-gravitating' leaves labelled with billiard balls are the same as those shown in Fig. 1. The 3D visualizations show position-position-velocity (p - p - v) space. RA, right ascension; dec., declination. For comparison with the ability of dendrograms (**c**) to track hierarchical structure, **d** shows a pseudo-dendrogram of the CLUMPFIND segmentation (**b**), with the same four labels used in Fig. 1 and in **a**. As 'clumps' are not allowed to belong to larger structures, each pseudo-branch in **d** is simply a series of lines connecting the maximum emission value in each clump to the threshold value. A very large number of clumps appears in **b** because of the sensitivity of CLUMPFIND to noise and small-scale structure in the data. In the online PDF version, the 3D cubes (**a** and **b**) can be rotated to any orientation, and surfaces can be turned on and off (interaction requires Adobe Acrobat version 7.0.8 or higher). In the printed version, the front face of each 3D cube (the 'home' view in the interactive online version) corresponds exactly to the patch of sky shown in Fig. 1, and velocity with respect to the Local Standard of Rest increases from front (-0.5 km s^{-1}) to back (8 km s^{-1}).

data, CLUMPFIND typically finds features on a limited range of scales, above but close to the physical resolution of the data, and its results can be overly dependent on input parameters. By tuning CLUMPFIND's two free parameters, the same molecular-line data set⁸ can be used to show either that the frequency distribution of clump mass is the same as the initial mass function of stars or that it follows the much shallower mass function associated with large-scale molecular clouds (Supplementary Fig. 1).

Four years before the advent of CLUMPFIND, 'structure trees'⁹ were proposed as a way to characterize clouds' hierarchical structure

using 2D maps of column density. With this early 2D work as inspiration, we have developed a structure-identification algorithm that abstracts the hierarchical structure of a 3D (p - p - v) data cube into an easily visualized representation called a 'dendrogram'¹⁰. Although well developed in other data-intensive fields^{11,12}, it is curious that the application of tree methodologies so far in astrophysics has been rare, and almost exclusively within the area of galaxy evolution, where 'merger trees' are being used with increasing frequency¹³.

Figure 3 and its legend explain the construction of dendrograms schematically. The dendrogram quantifies how and where local maxima of emission merge with each other, and its implementation is explained in Supplementary Methods. Critically, the dendrogram is determined almost entirely by the data itself, and it has negligible sensitivity to algorithm parameters. To make graphical presentation possible on paper and 2D screens, we 'flatten' the dendrograms of 3D data (see Fig. 3 and its legend), by sorting their 'branches' to not cross, which eliminates dimensional information on the x axis while preserving all information about connectivity and hierarchy. Numbered 'billiard ball' labels in the figures let the reader match features between a 2D map (Fig. 1), an interactive 3D map (Fig. 2a online) and a sorted dendrogram (Fig. 2c).

A dendrogram of a spectral-line data cube allows for the estimation of key physical properties associated with volumes bounded by isosurfaces, such as radius (R), velocity dispersion (σ_v) and luminosity (L). The volumes can have any shape, and in other work¹⁴ we focus on the significance of the especially elongated features seen in L1448 (Fig. 2a). The luminosity is an approximate proxy for mass, such that $M_{\text{lum}} = X_{^{13}\text{CO}} L_{^{13}\text{CO}}$, where $X_{^{13}\text{CO}} = 8.0 \times 10^{20} \text{ cm}^2 \text{ K}^{-1} \text{ s}$ (ref. 15; see Supplementary Methods and Supplementary Fig. 2). The derived values for size, mass and velocity dispersion can then be used to estimate the role of self-gravity at each point in the hierarchy, via calculation of an 'observed' virial parameter, $\alpha_{\text{obs}} = 5\sigma_v^2 R/GM_{\text{lum}}$. In principle, extended portions of the tree (Fig. 2, yellow highlighting) where $\alpha_{\text{obs}} < 2$ (where gravitational energy is comparable to or larger than kinetic energy) correspond to regions of p - p - v space where self-gravity is significant. As α_{obs} only represents the ratio of kinetic energy to gravitational energy at one point in time, and does not explicitly capture external over-pressure and/or magnetic fields¹⁶, its measured value should only be used as a guide to the longevity (boundedness) of any particular feature.

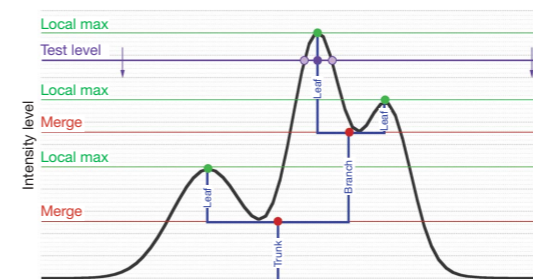
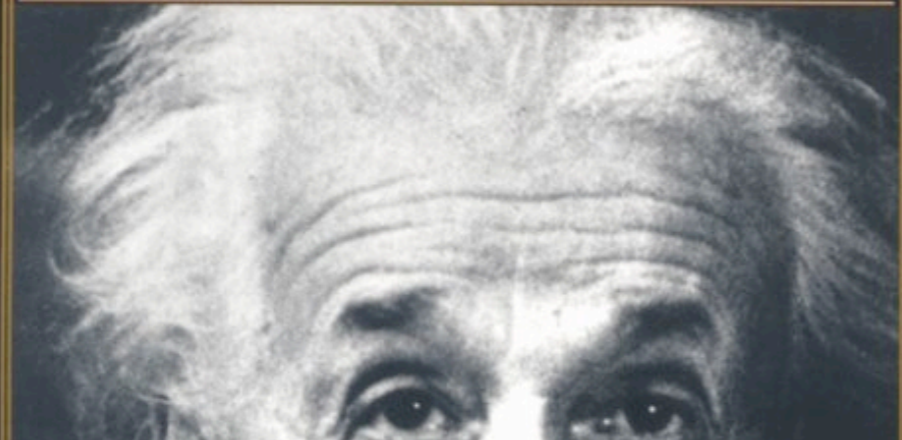


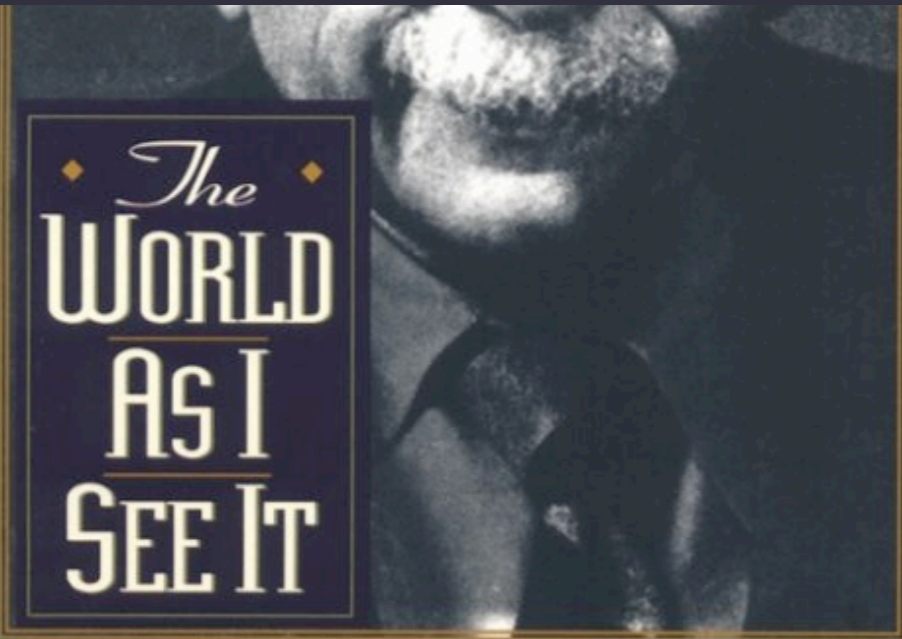
Figure 3 | Schematic illustration of the dendrogram process. Shown is the construction of a dendrogram from a hypothetical one-dimensional emission profile (black). The dendrogram (blue) can be constructed by 'dropping' a test constant emission level (purple) from above in tiny steps (exaggerated in size here, light lines) until all the local maxima and mergers are found, and connected as shown. The intersection of a test level with the emission is a set of points (for example the light purple dots) in one dimension, a planar curve in two dimensions, and an isosurface in three dimensions. The dendrogram of 3D data shown in Fig. 2c is the direct analogue of the tree shown here, only constructed from 'isosurface' rather than 'point' intersections. It has been sorted and flattened for representation on a flat page, as fully representing dendrograms for 3D data cubes would require four dimensions.

ALBERT EINSTEIN



The most incomprehensible

“Astronomy as I See It”



- Albert Einstein

Relative Strengths



Pattern Recognition
Creativity



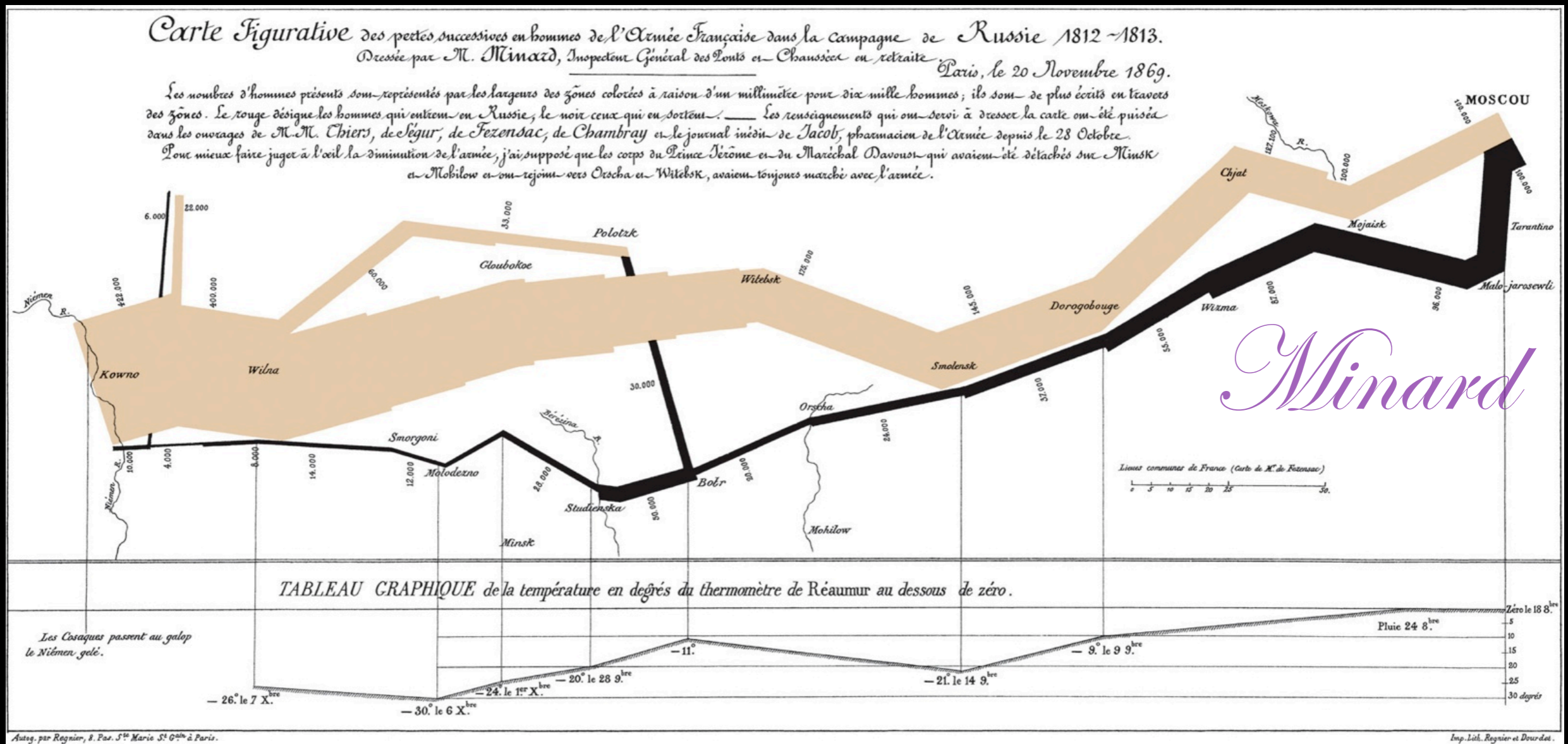
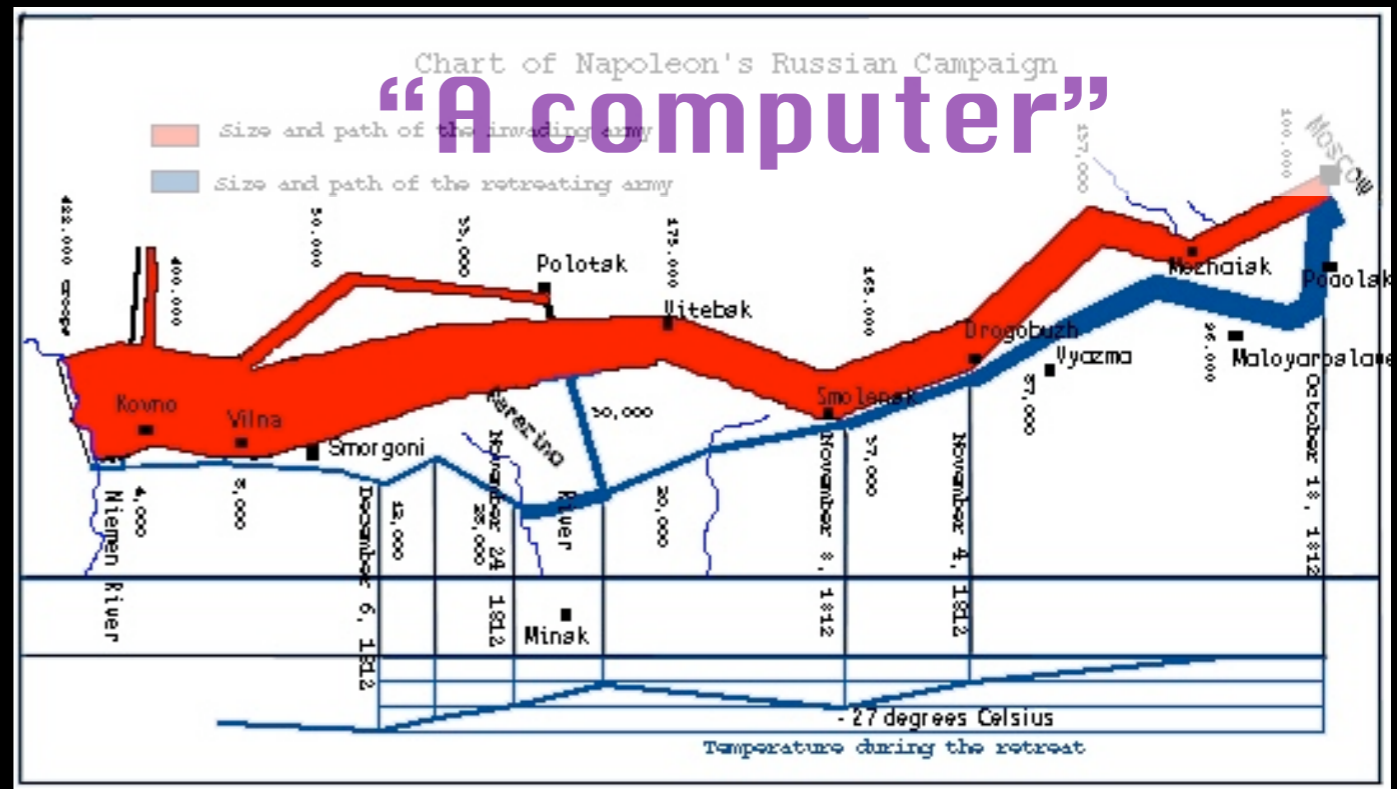
Calculations



“Interocularity”
(see work of John Tukey)

“Image and Meaning”
(see work of Felice Frankel,
and imageandmeaning.org)

Are we held back by
confining
technological tools?



Galileo, Science & Technology

Sex^{mo} Principe.

Galileo Galilei, Humilis^s Servus della Ser.^a V.^a inuigilanti
 et assiduam et ad ogni spirito di bere non solo satisfatto
 alvario che non della stessa di Matematicis nelle Scuole
 di Padova,

Inuigilanti determinati di presentare al Sex^{mo} Principe
 l'occhio et di essere di giuramento inestimabile di ogni
 negozio et in ogni marittima o terrestre strada di tenere per
 questo nuovo artificio ne l'ingegno segreto et solam a disposizione
 di l'occhio l'occhio conato dalle più re d'ite speculazioni di
 prospettiva in l'quantaggio di scoprire Legni et Vele dell'inimico
 di l'occhio et di più di tempo prima di essi sopra noi et distinguendo
 il numero et la qualità dei Vasselli giudicare le sue forze
 ballastarsi alla caccia al combattimento o alla fuga, o pure essi
 nella campagna aperta vedere et particolarmente distinguere ogni suo
 moto et proporzionamento.

Adi 7. di gennaio
 Giove si vide a 7^o * * * * *

Adi 8. di
 4 * * * * * ora d'ora diretto et non retrogrado

Adi 12. di adda in tale costituzione * * * * *

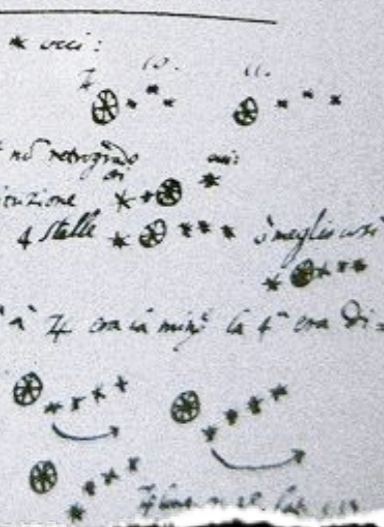
Adi 13. di adda in tal modo a Giove 4 stelle * * * * *

Adi 14. di agosto
 11 * * * * * la pressi a 4 ora in migli la 4^a ora di =

stante dalla 3^a l'occhio l'occhio

La spatio delle 3 meridionali ad om
 maggiore del diametro di 7 et c =

ora in linea retta.



7	* * ○ *	17	* ○
8	○ * * *	18	* ○
10	* * ○	19	* ○ * *
11	* * ○	19	* ○ * *
12	* ○ *	20	○ * ○ ○
13	* ○ * *	21	○ * *
15	○ * * *	22	* ○ * *
15	○ * * *	22	○ * * *
16	○ * *	23	* ○ * *
17	* ○ *	24	* ○ * *
		24	* ○

SIDERIUS NUNCIUS

On the third, at the seventh hour, the stars were arranged in this
 quence. The eastern one was 1 minute, 30 seconds from Jupiter
 the closest western one 2 minutes; and the other western one wa

East * ○ * * West

10 minutes removed from this one. They were absolutely on the
 same straight line and of equal magnitude.

On the fourth, at the second hour, there were four stars around
 Jupiter, two to the east and two to the west, and arranged precise

East * * ○ * * West

on a straight line, as in the adjoining figure. The easternmost wa
 distant 3 minutes from the next one, while this one was 40 second
 from Jupiter; Jupiter was 4 minutes from the nearest western one
 and this one 6 minutes from the westernmost one. Their magnitude,
 were nearly equal; the one closest to Jupiter appeared a little smaller
 than the rest. But at the seventh hour the eastern stars were only
 10 seconds apart. Jupiter was 2 minutes from the nearer eastern

East ** ○ * * West

one, while he was 4 minutes from the next western one, and this
 one was 3 minutes from the westernmost one. They were all equal
 and extended on the same straight line along the ecliptic.

On the fifth, the sky was cloudy.

On the sixth, only two stars appeared flanking Jupiter, as is seen

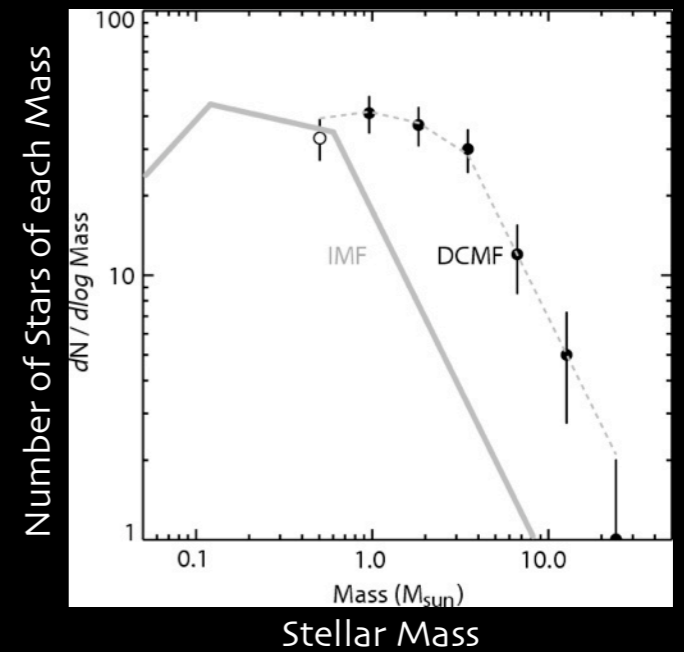
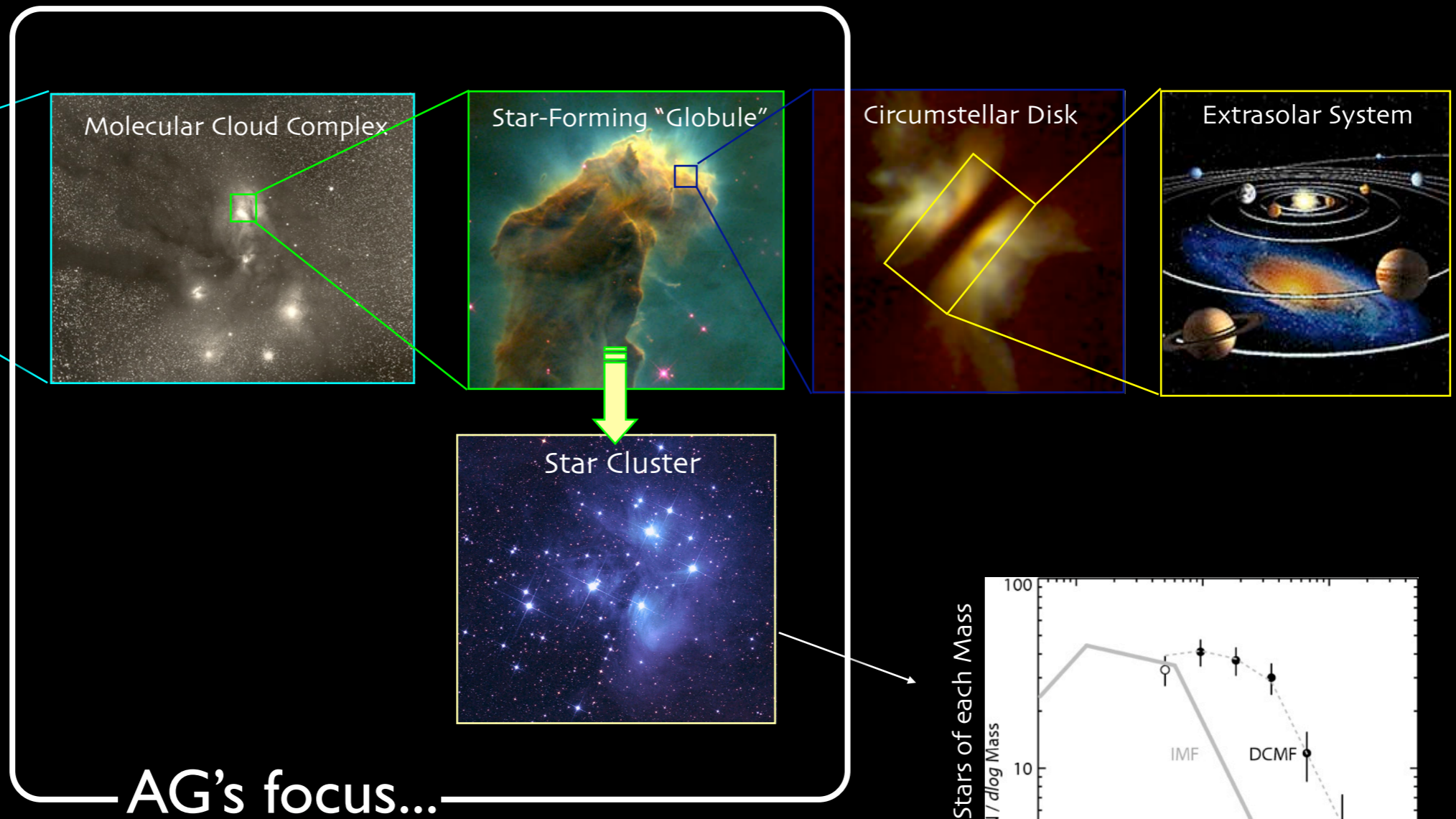
East * ○ * West

in the adjoining figure. The eastern one was 2 minutes and the
 western one 3 minutes from Jupiter. They were on the same straight
 line with Jupiter and equal in magnitude.

On the seventh, two stars stood near Jupiter, both to the east

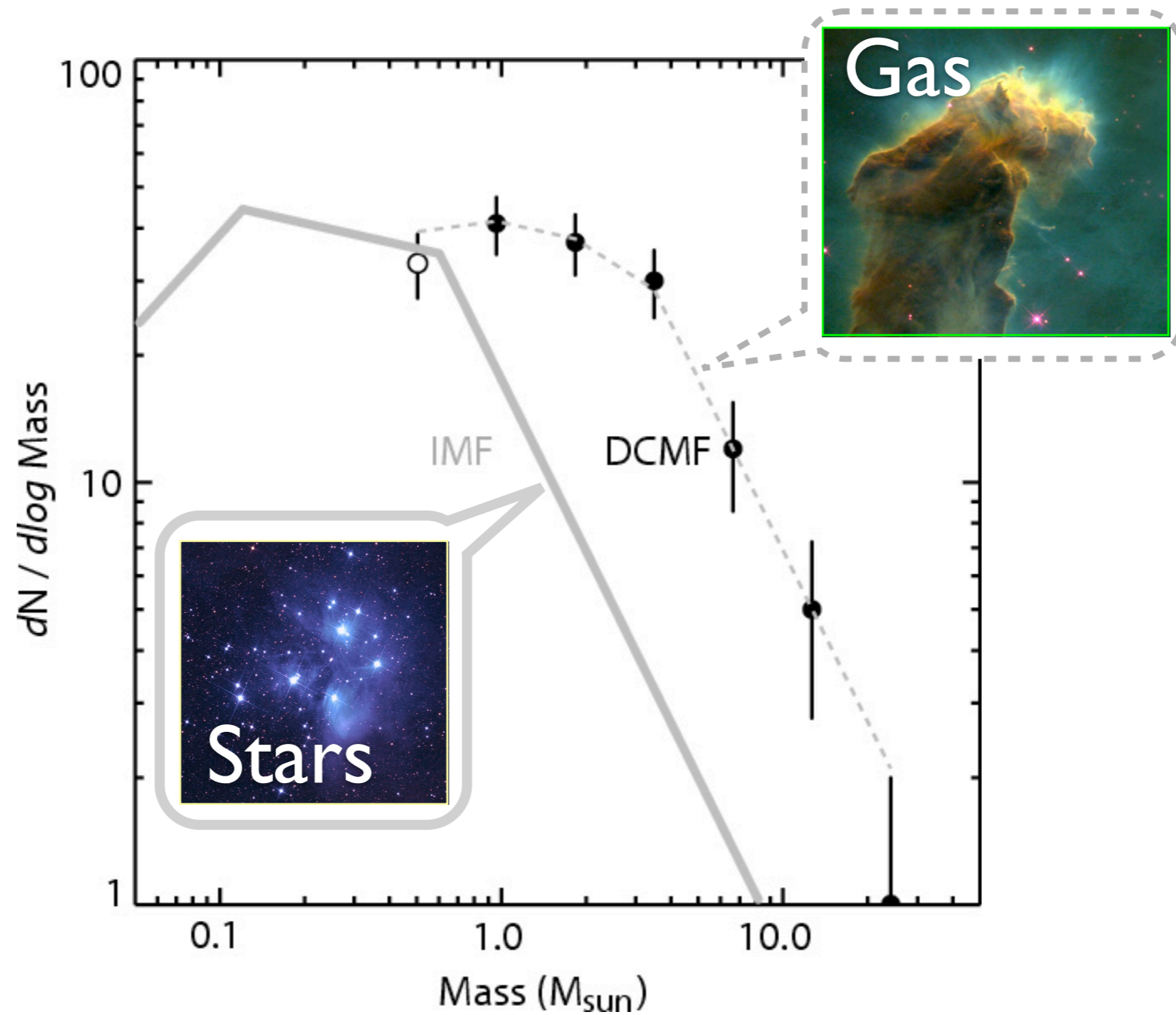
Notes for & re-productions of Siderius Nuncius (1610)

Star (and Planet, and Moon) Formation 101



“IMF”? “CMF”?

Note: IMF= “Initial Mass Function” of Stars, not “International Monetary Fund.”



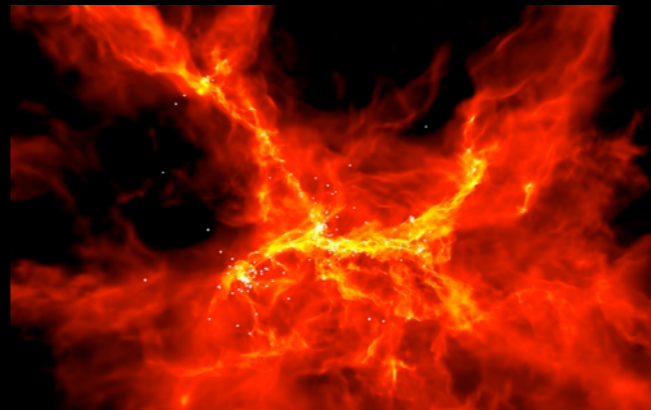
Alves, Lombardi & Lada 2007

Gas

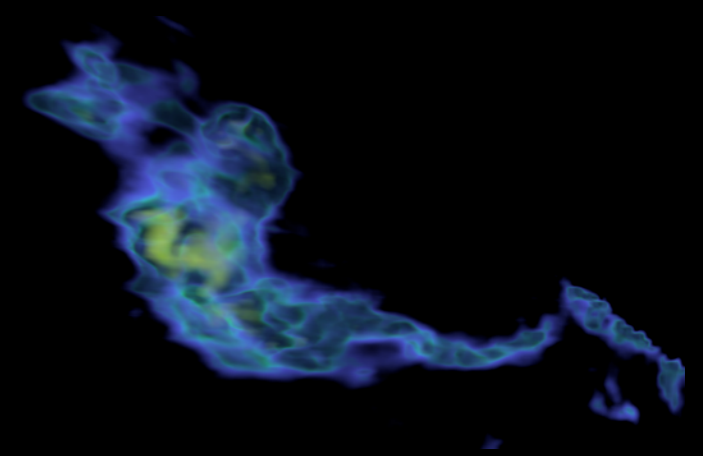


BUT: Beautiful images like this do not reveal *internal* structure directly...

simulations



>2D
observations





Astronomical Medicine

Alyssa Goodman (IIC/CfA/FAS)

Michael Halle (IIC/SPL/HMS)

Ron Kikinis (SPL/HMS)

Douglas Alan (IIC)

Michelle Borkin (FAS/IIC)

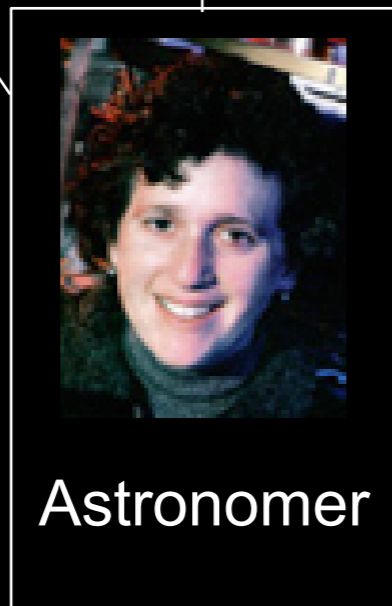
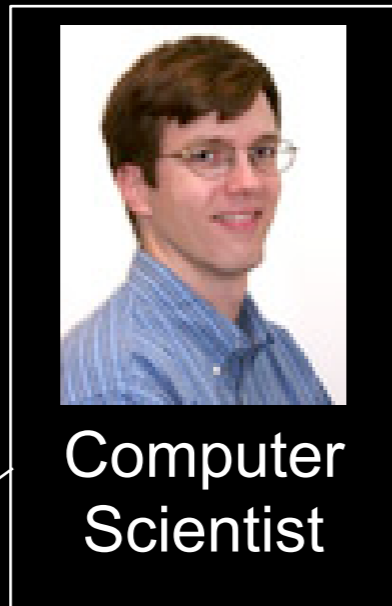
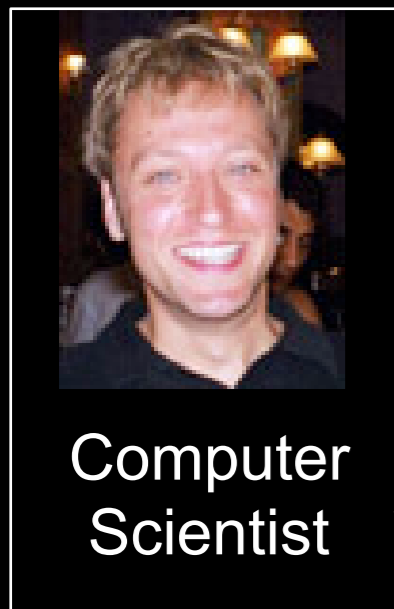
Jens Kauffmann (CfA/IIC)

Erik Rosolowsky (CfA/UBC Okanagan)

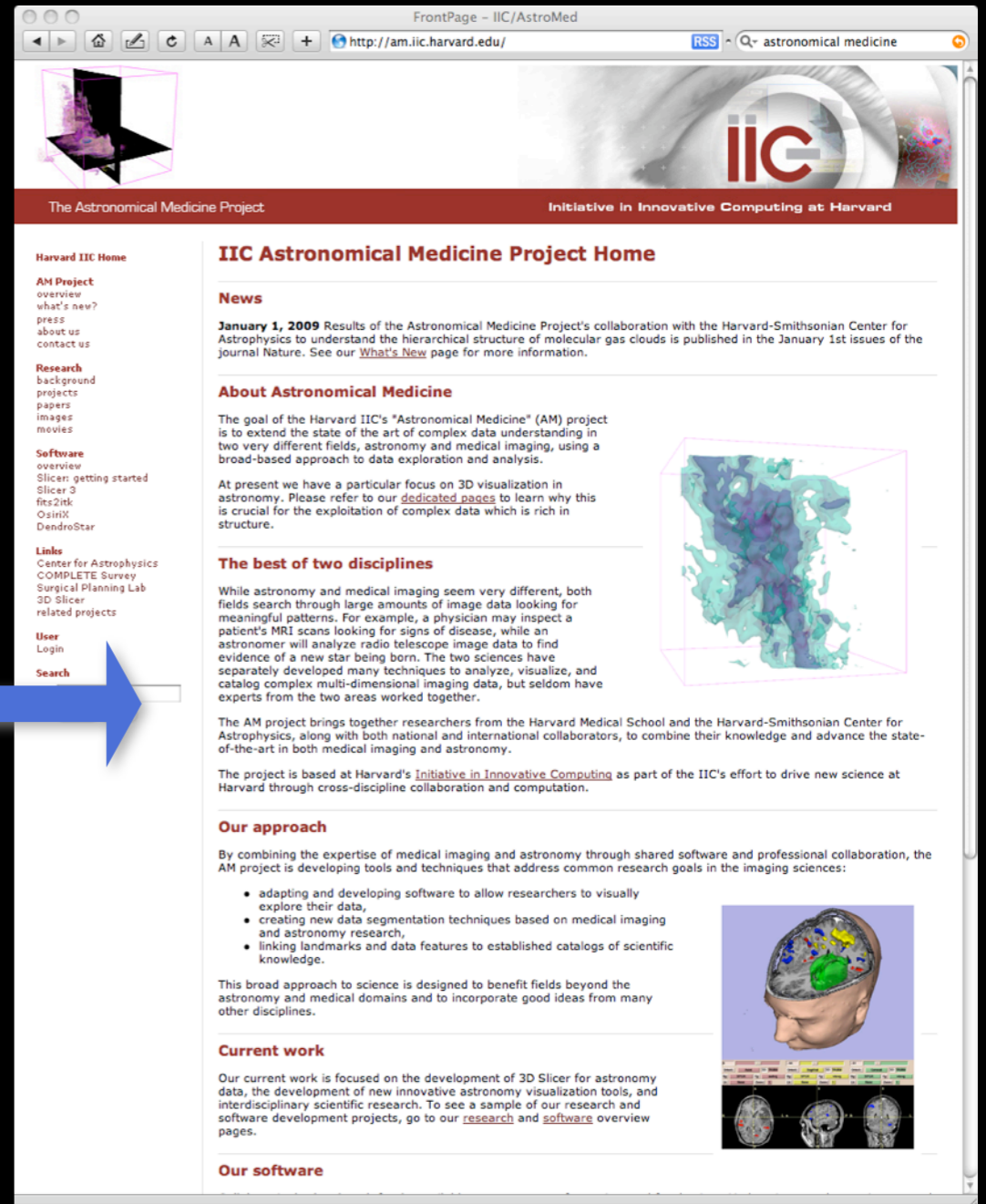
Nick Holliman (U. Durham)



The Astronomical Medicine Story







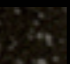
“Viz has failed the scientific community...”

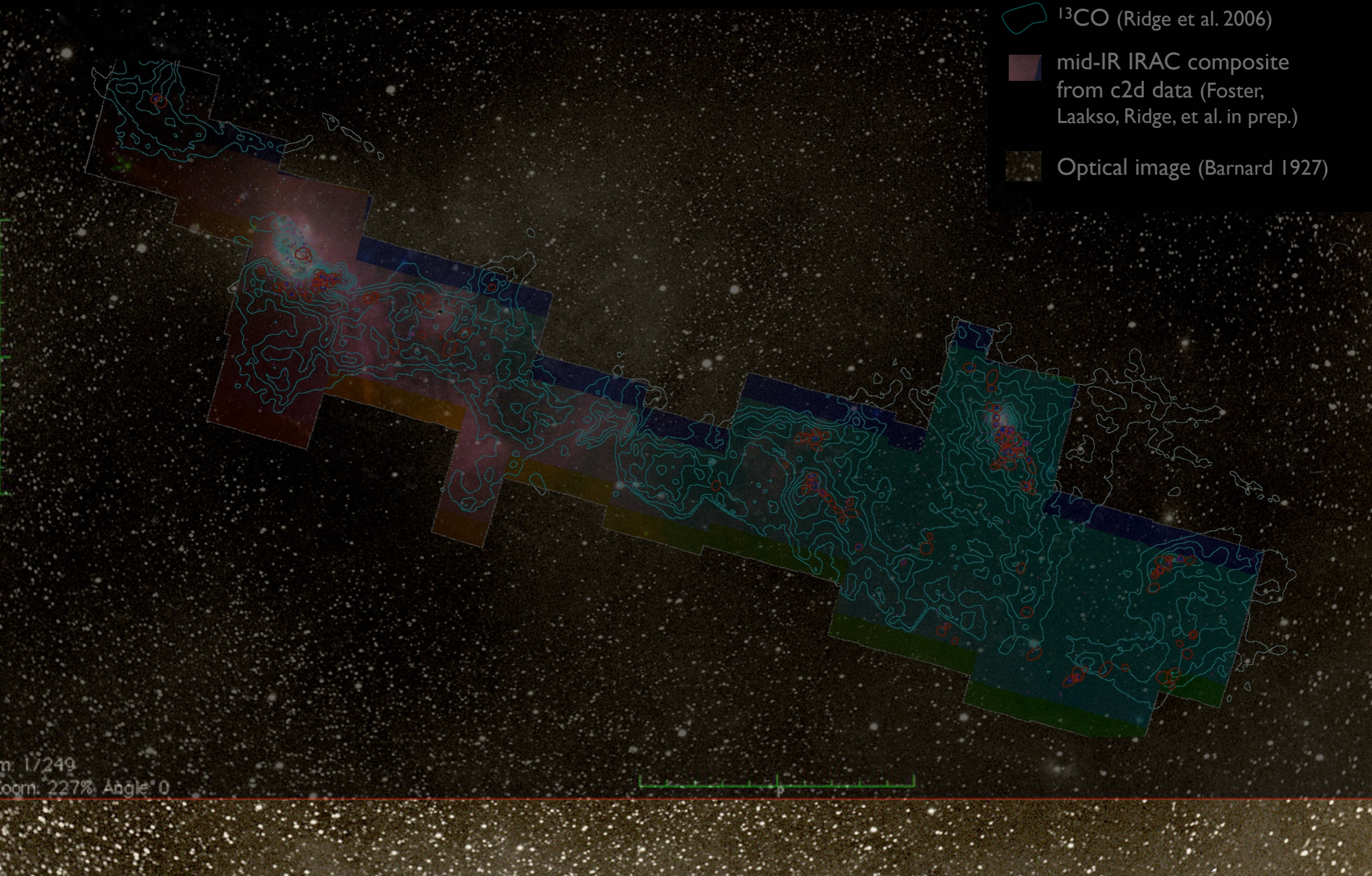


- +Nick Holliman (CS, 3D expert)
- +Doug Alan (S/W Engineer)
- +Jens Kauffmann (postdoc)
- +Erik Rosolowsky (postdoc) + ...



COMPLETE = COordinated Molecular Probe Line Exinction Thermal Emission

-  mm peak (Enoch et al. 2006)
-  sub-mm peak (Hatchell et al. 2005, Kirk et al. 2006)
-  ^{13}CO (Ridge et al. 2006)
-  mid-IR IRAC composite from c2d data (Foster, Laakso, Ridge, et al. in prep.)
-  Optical image (Barnard 1927)

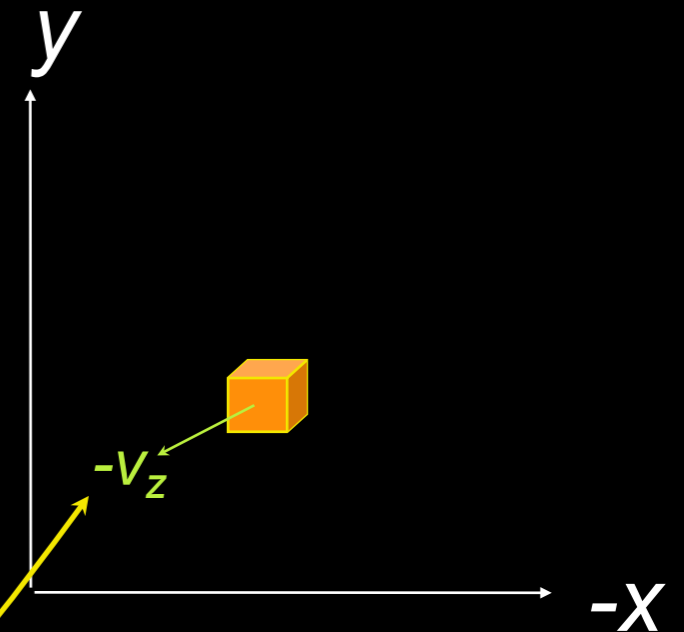
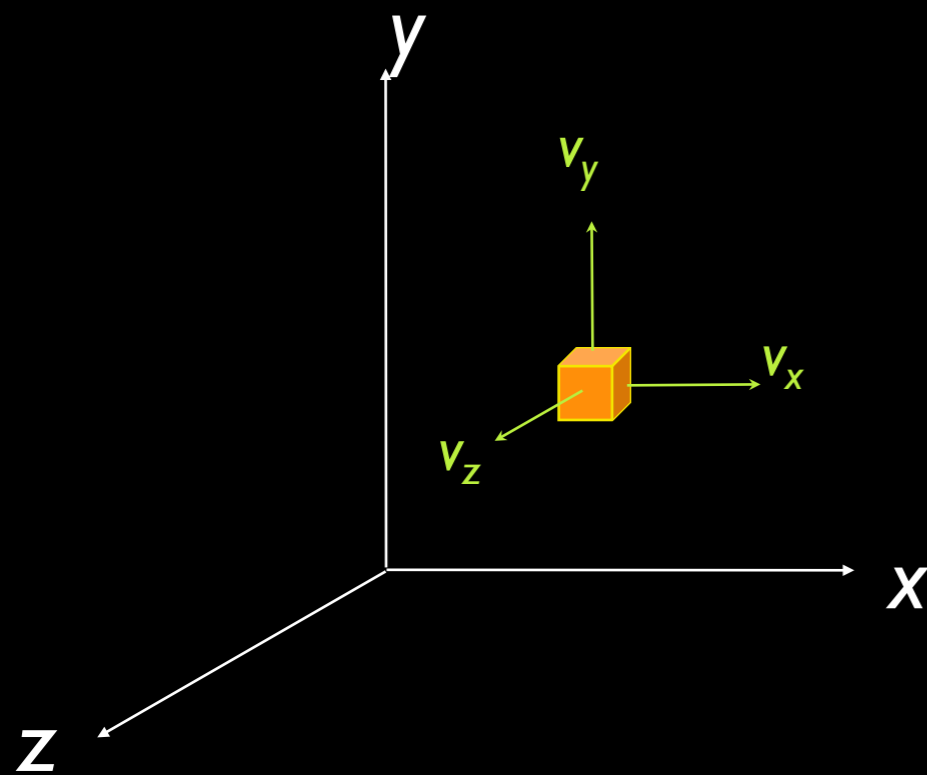


m: 1/249
Zoom: 227% Angle: 0

“Three” Dimensions: Spectral-Line Mapping

We wish we could measure...

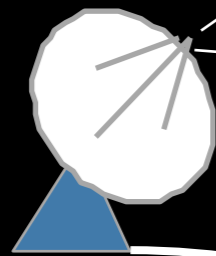
But we can measure...



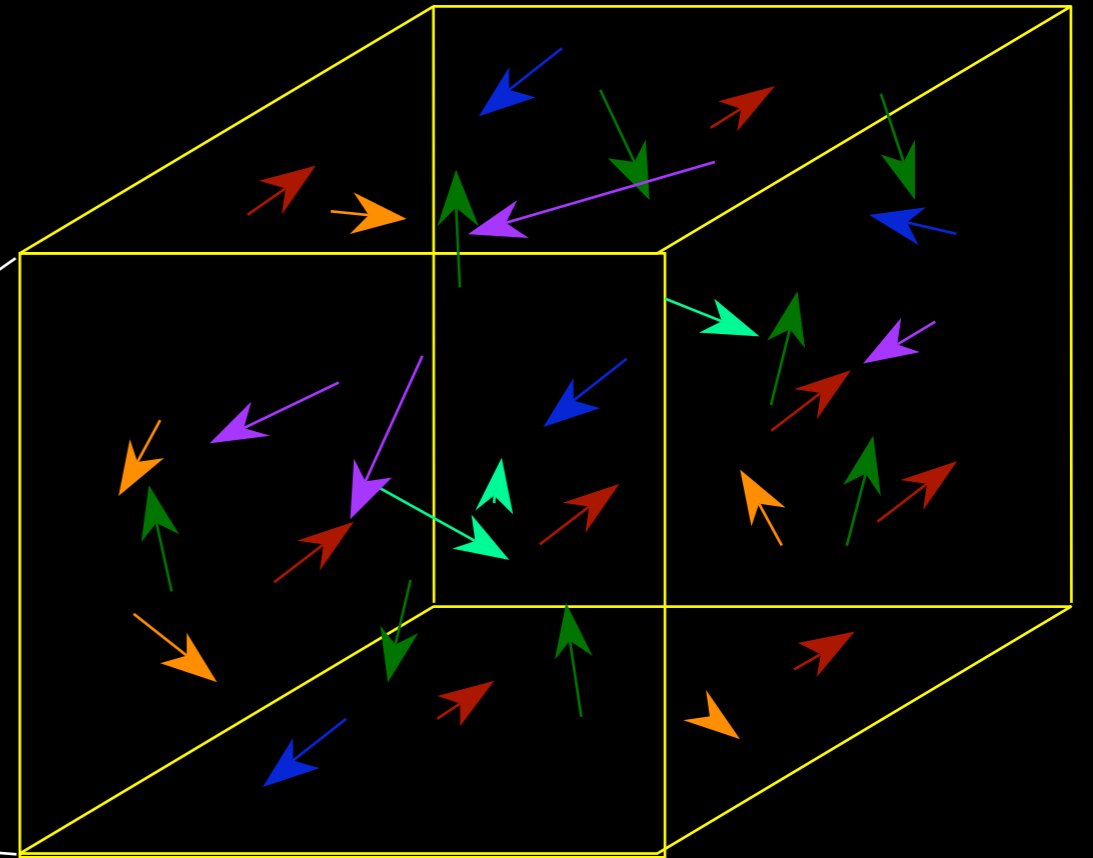
v_z *only* from
“spectral-line
maps”



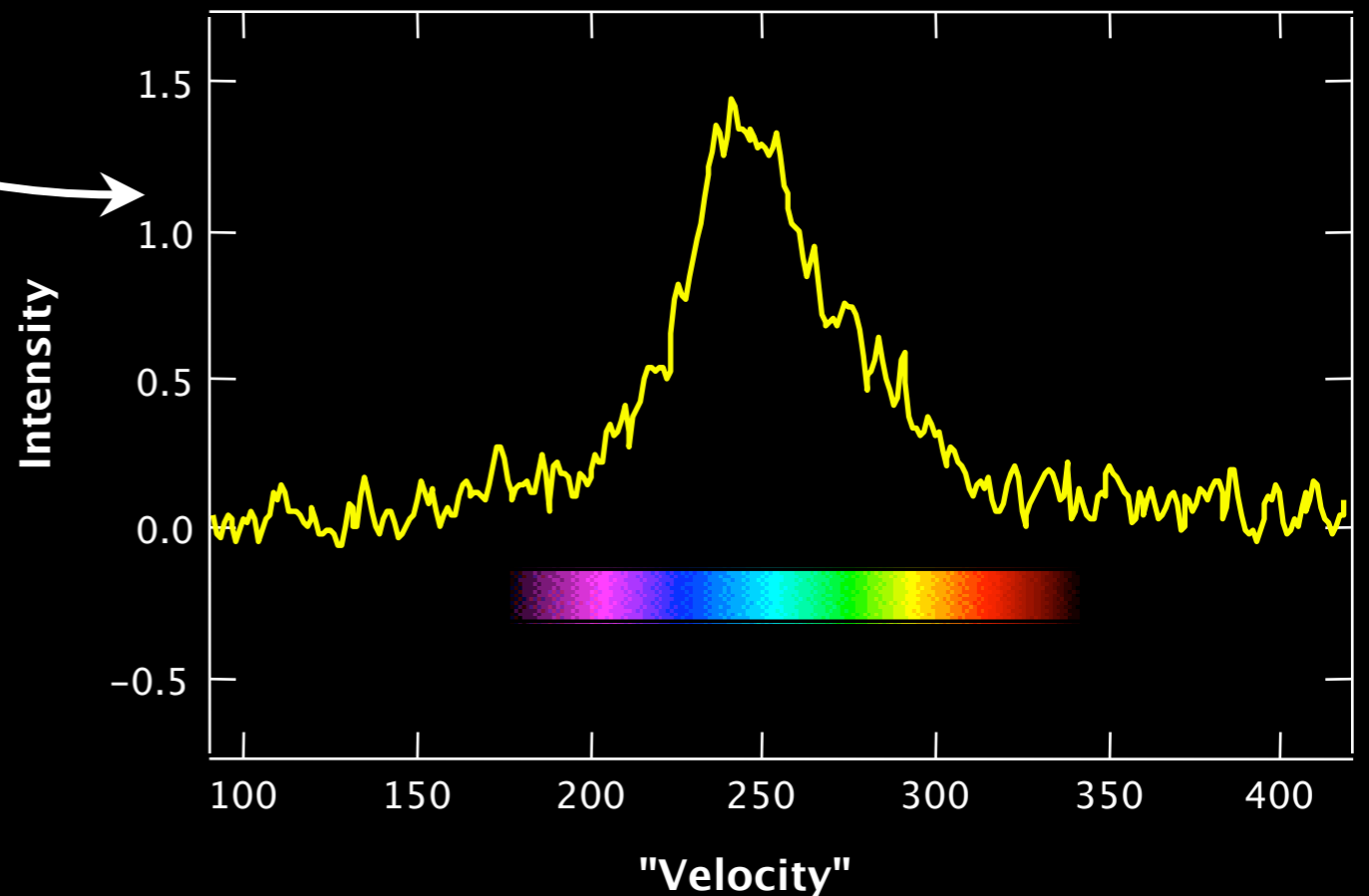
Velocity from Spectroscopy



Telescope +
Spectrometer

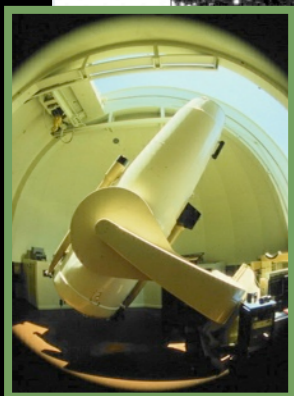
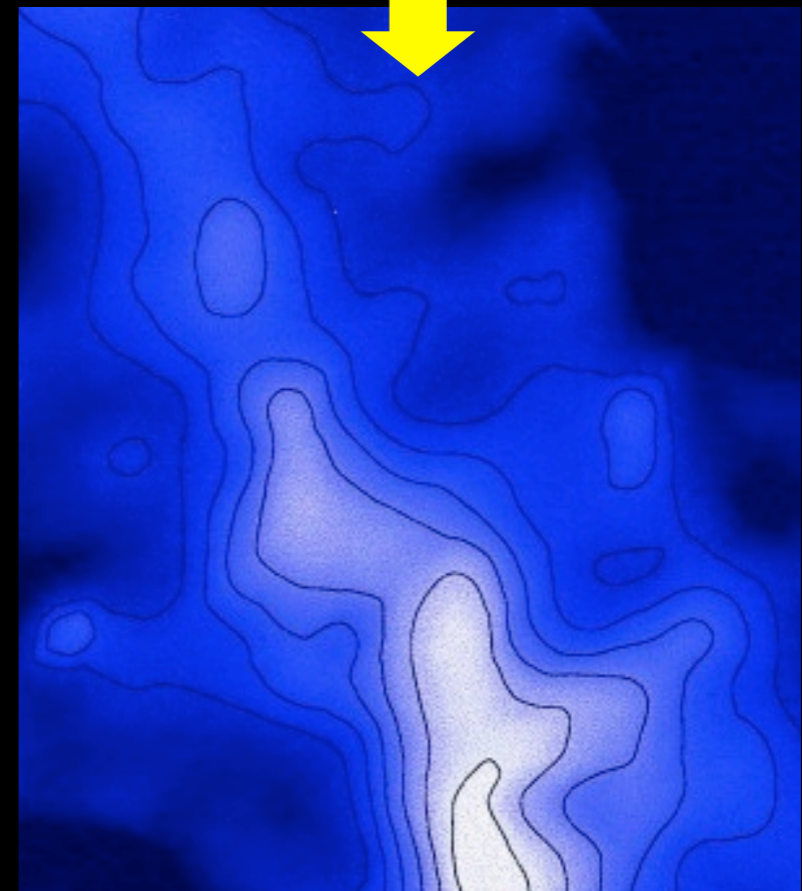
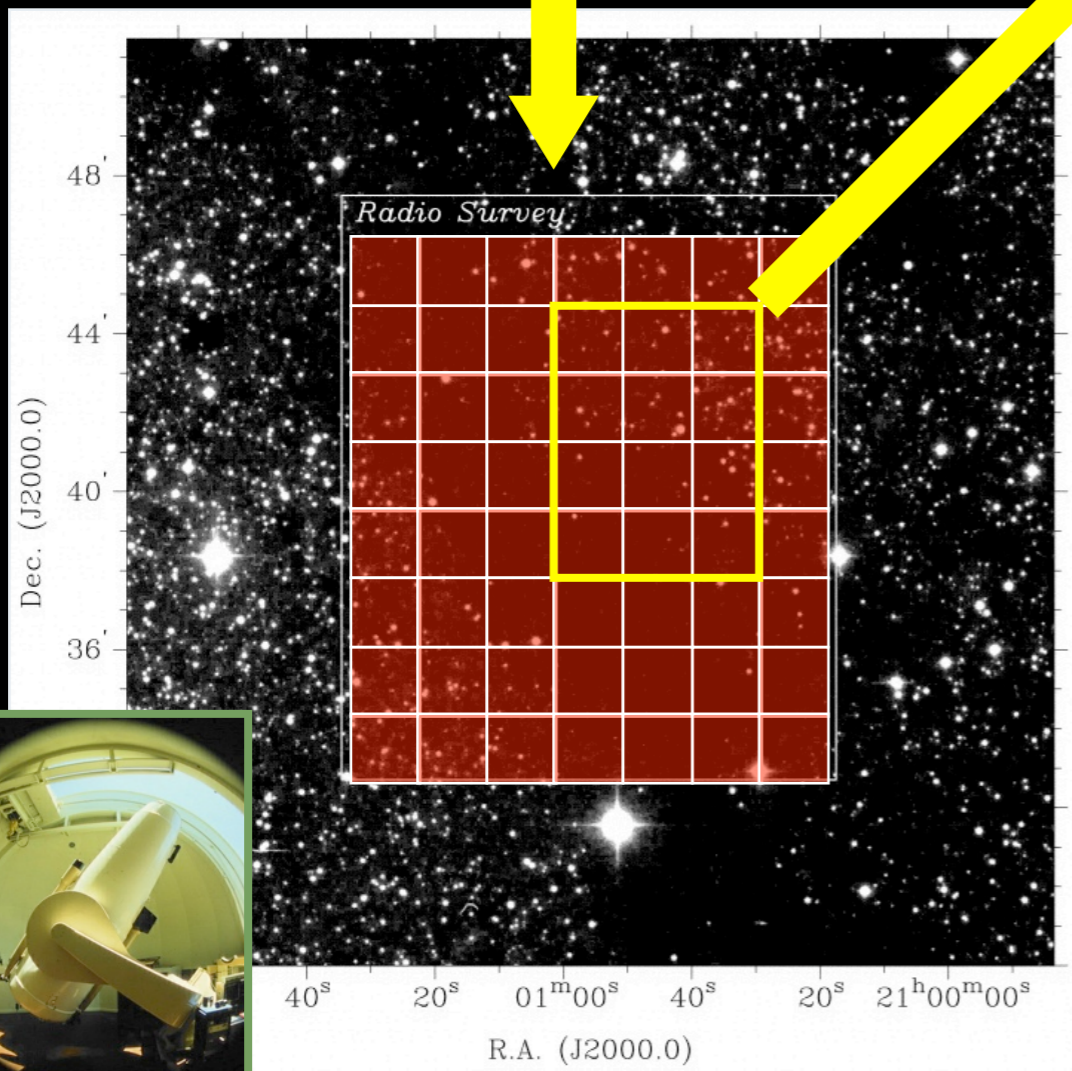
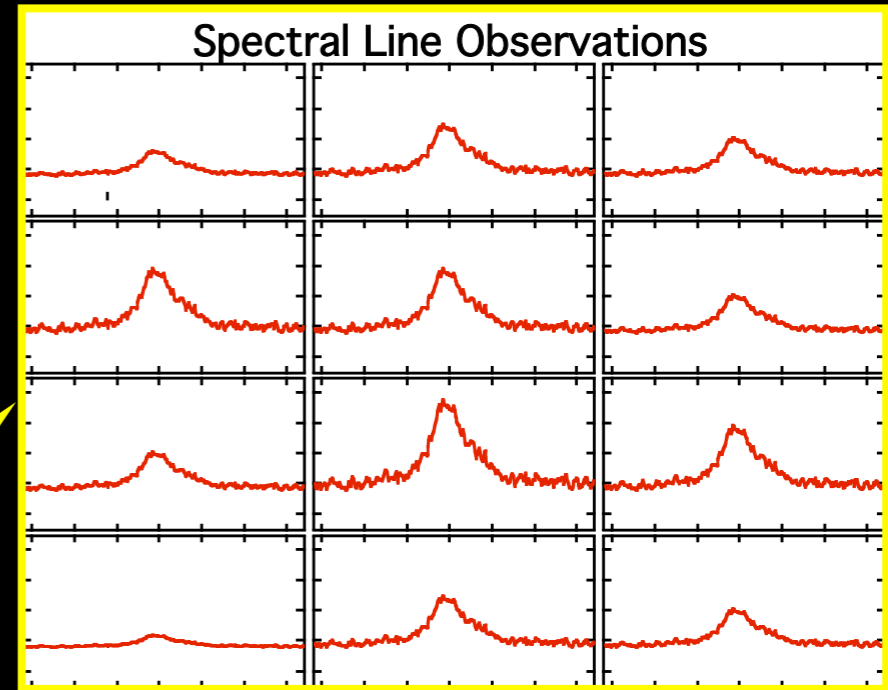


Observed Spectrum

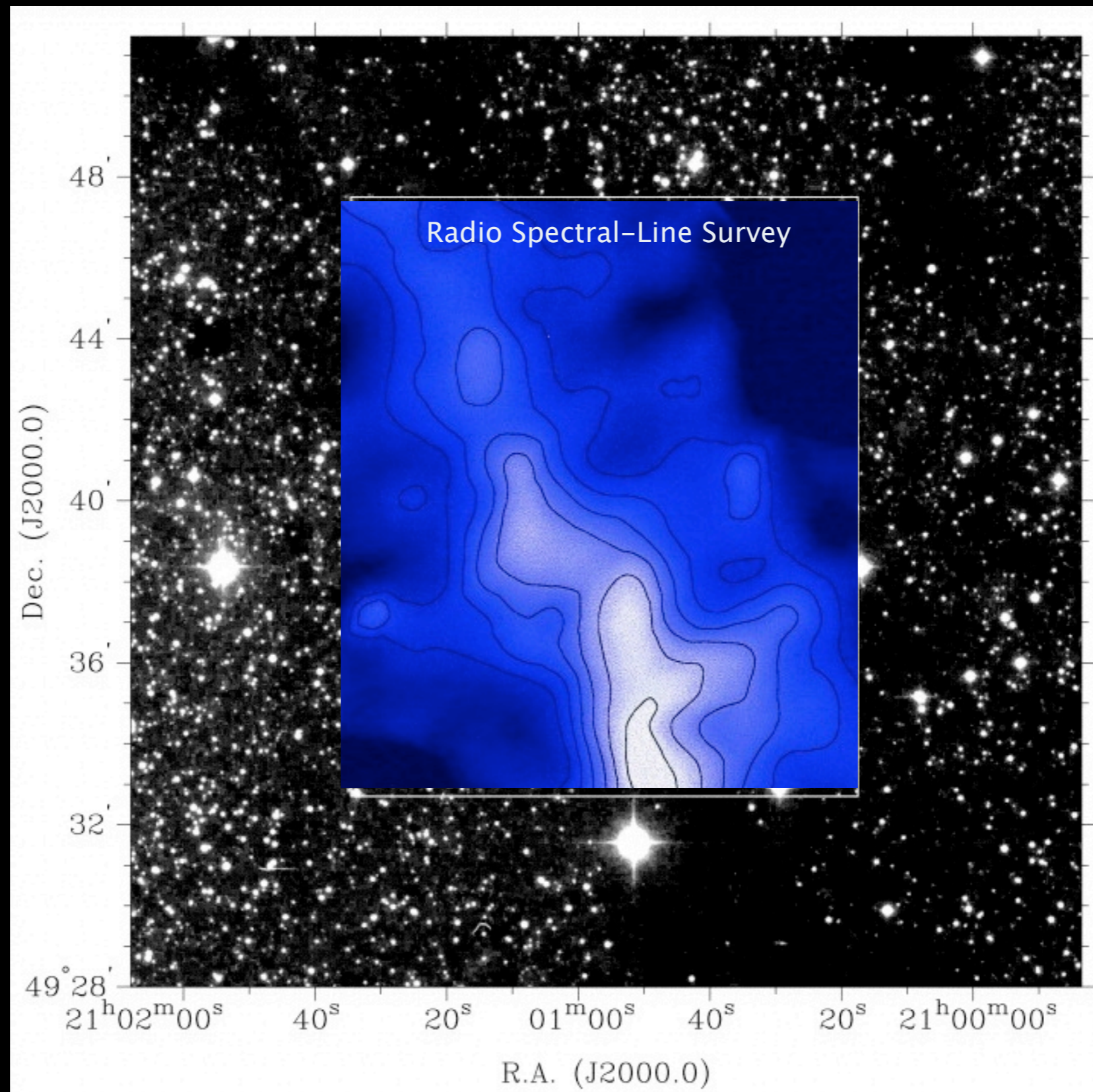


All thanks to Doppler

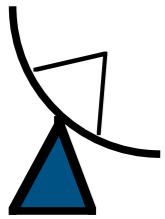
Radio Spectral-line Observations of Interstellar Clouds



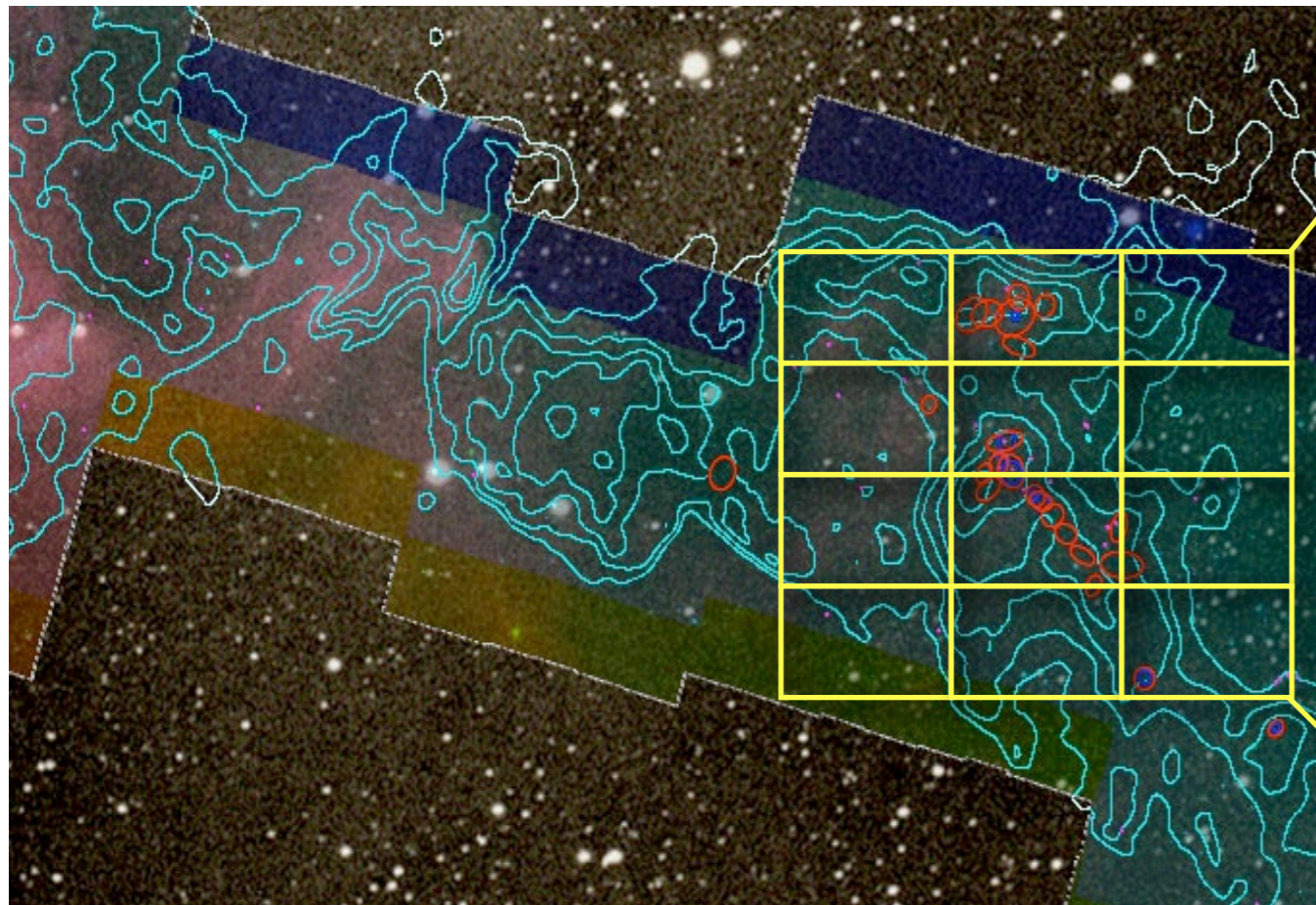
Radio Spectral-line Observations of Interstellar Clouds



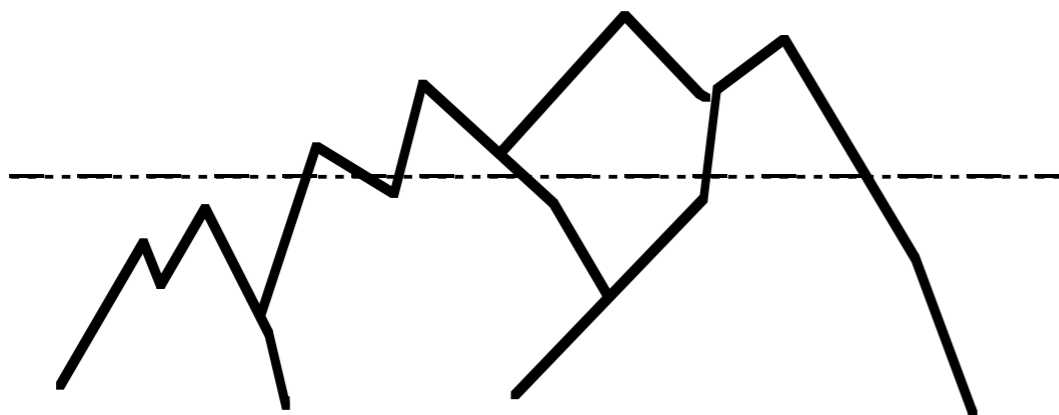
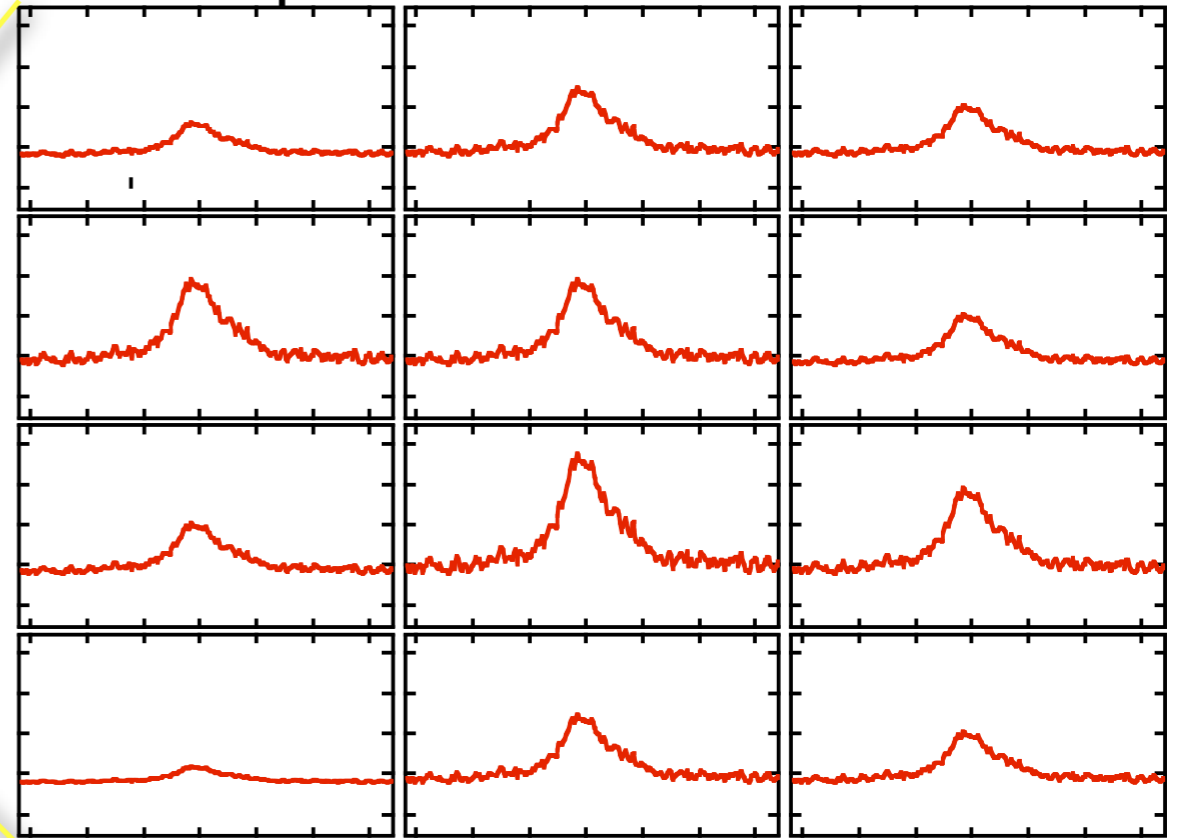
Alves, Lada & Lada 1999



Velocity as a "Fourth" Dimension



Spectral Line Observations



Mountain Range



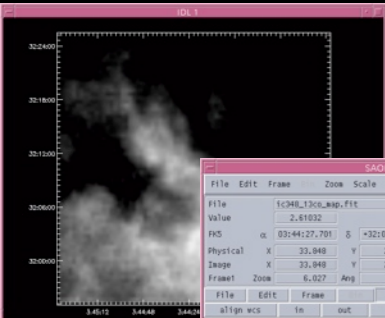
No loss of information



Loss of 1 dimension

Astronomical Visualization Tools are Traditionally 2D

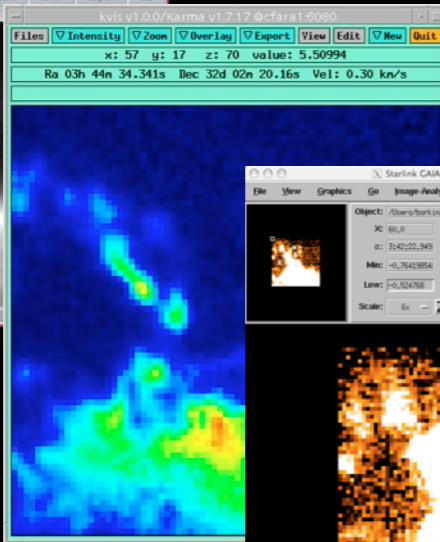
IDL



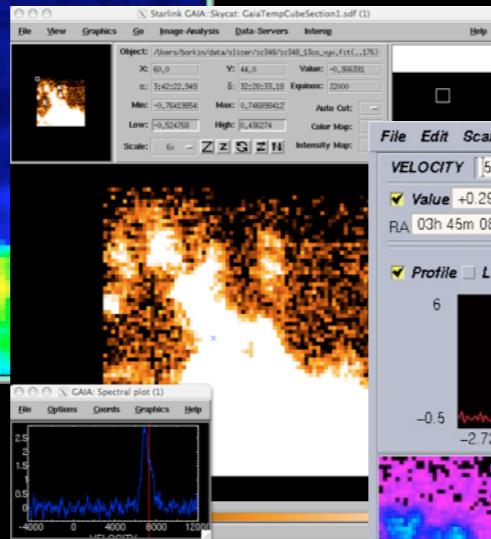
DS9



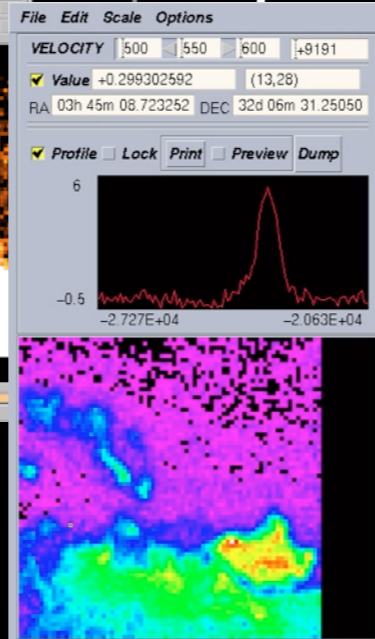
Karma*



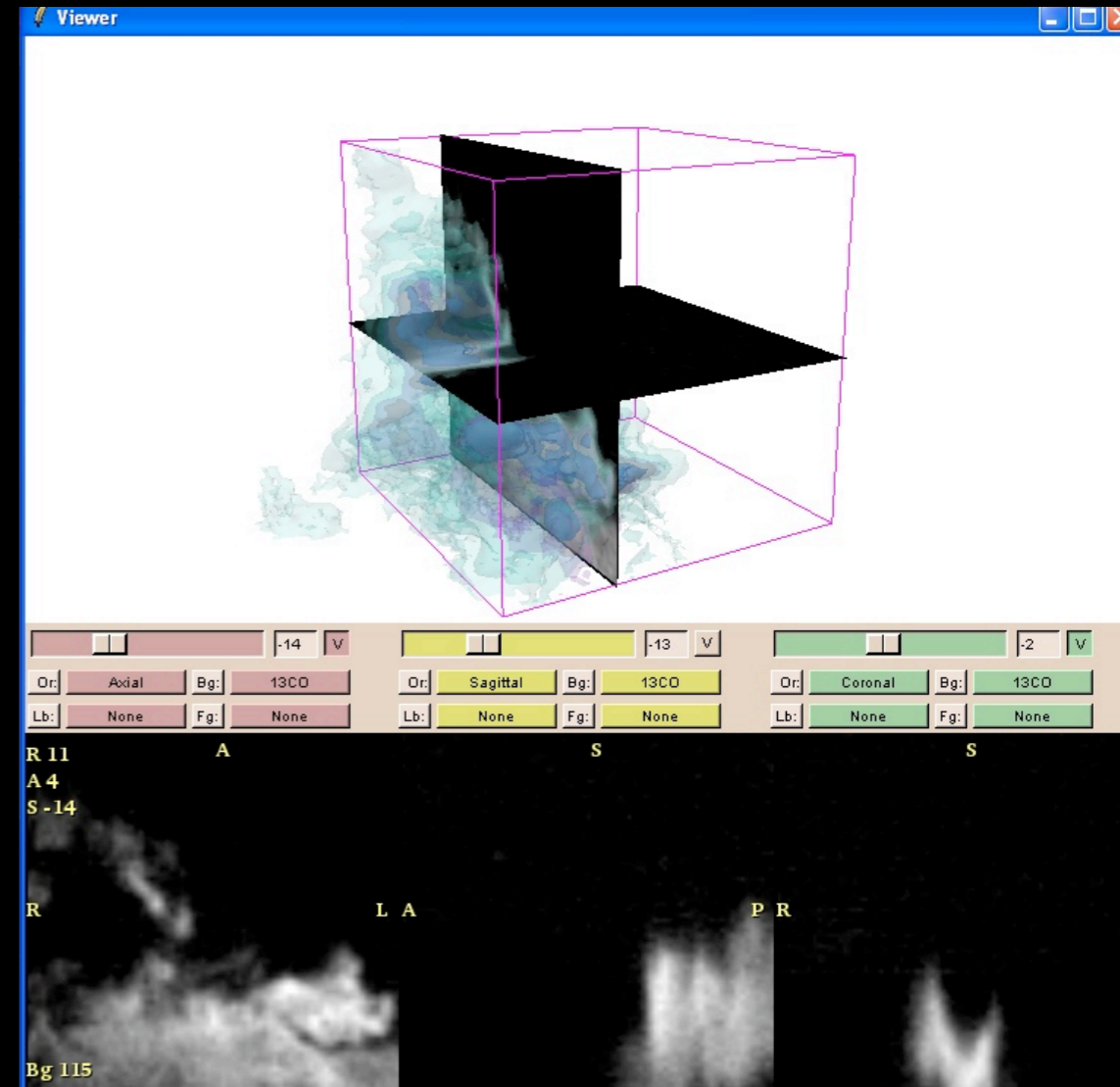
GAIA



Aipsview



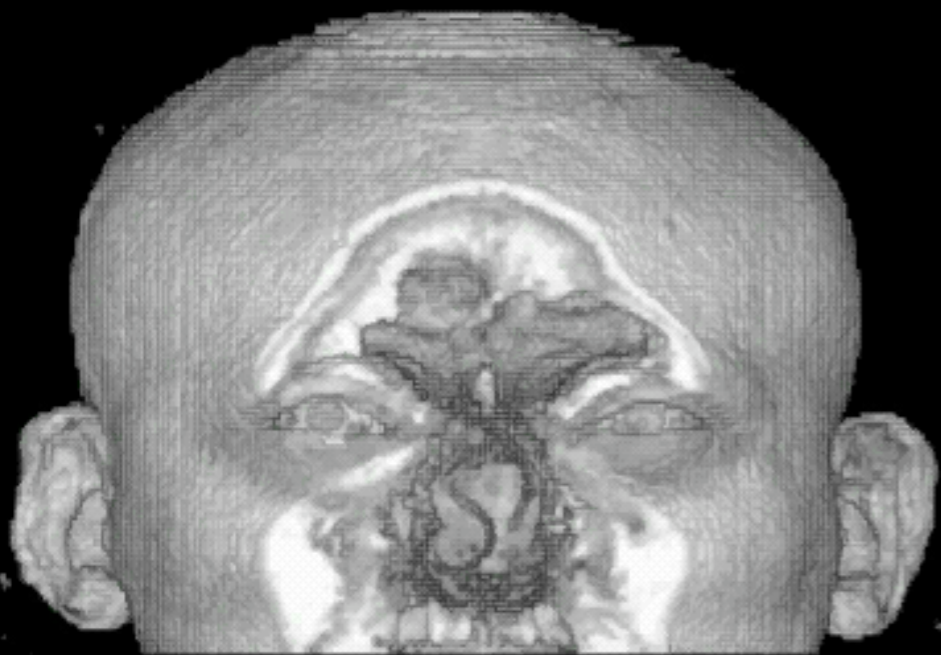
3D Slicer



“3D”=movies

“Astronomical Medicine”

“KEITH”



“z” is depth into head

“PERSEUS”

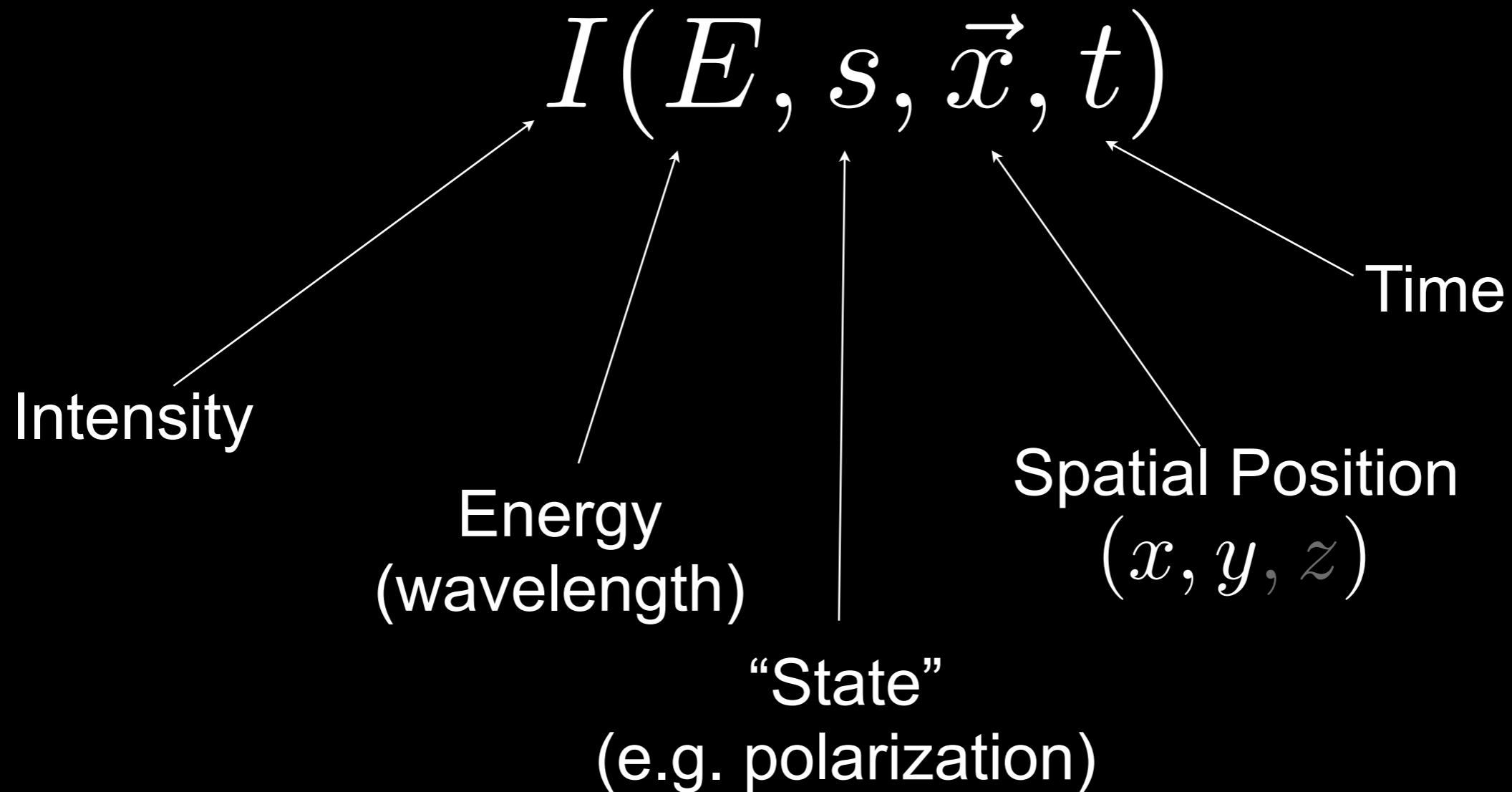


“z” is line-of-sight velocity

(This kind of “series of 2D slices view” is known in the Viz as “the grand tour”)

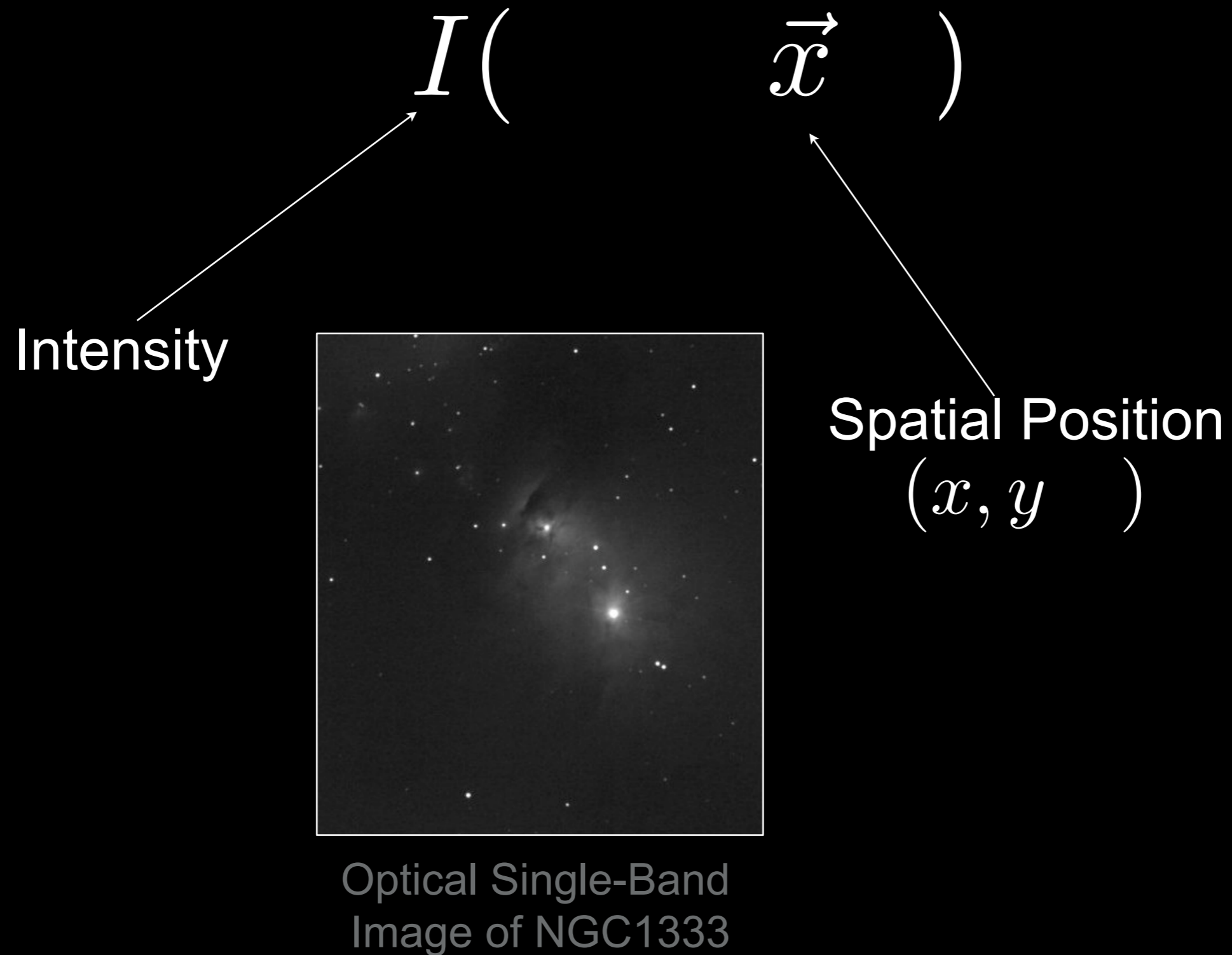


What can we observe?

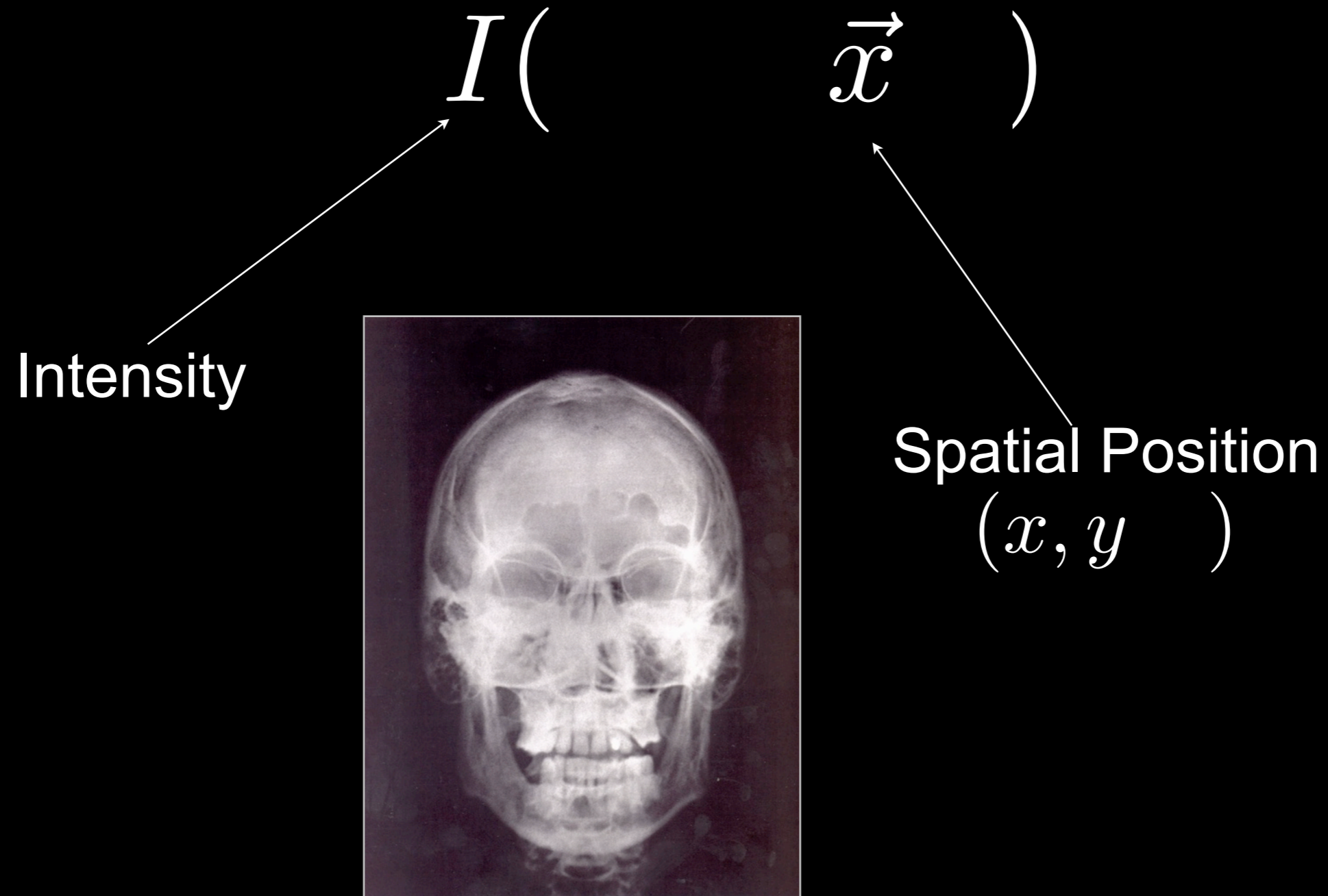


...and the science is in the interpretation of these measurements into physical quantities & processes.

What can we observe?



What can we observe?



X-Ray of Human Skull, c. 1920

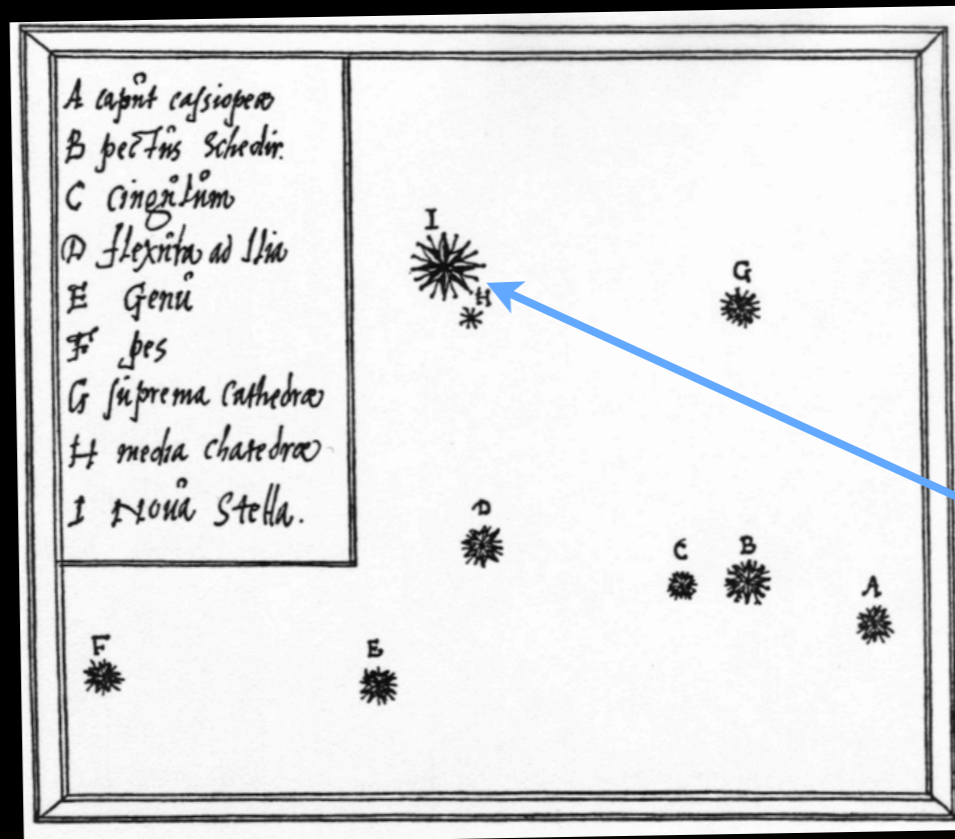
What can we observe?

$$I(\vec{x}, t)$$

Intensity

Time

Spatial Position
(x, y, z)



“Nova Stella”
of Tycho, 1572

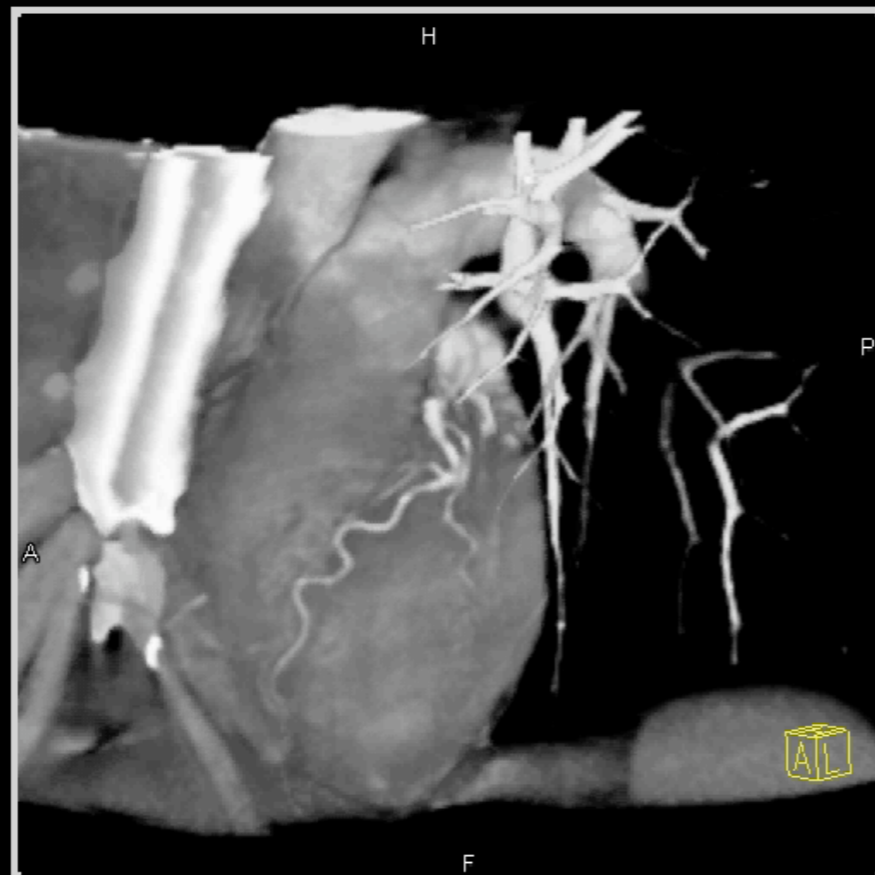
What can we observe?

$$I(\vec{x}, t)$$

Intensity

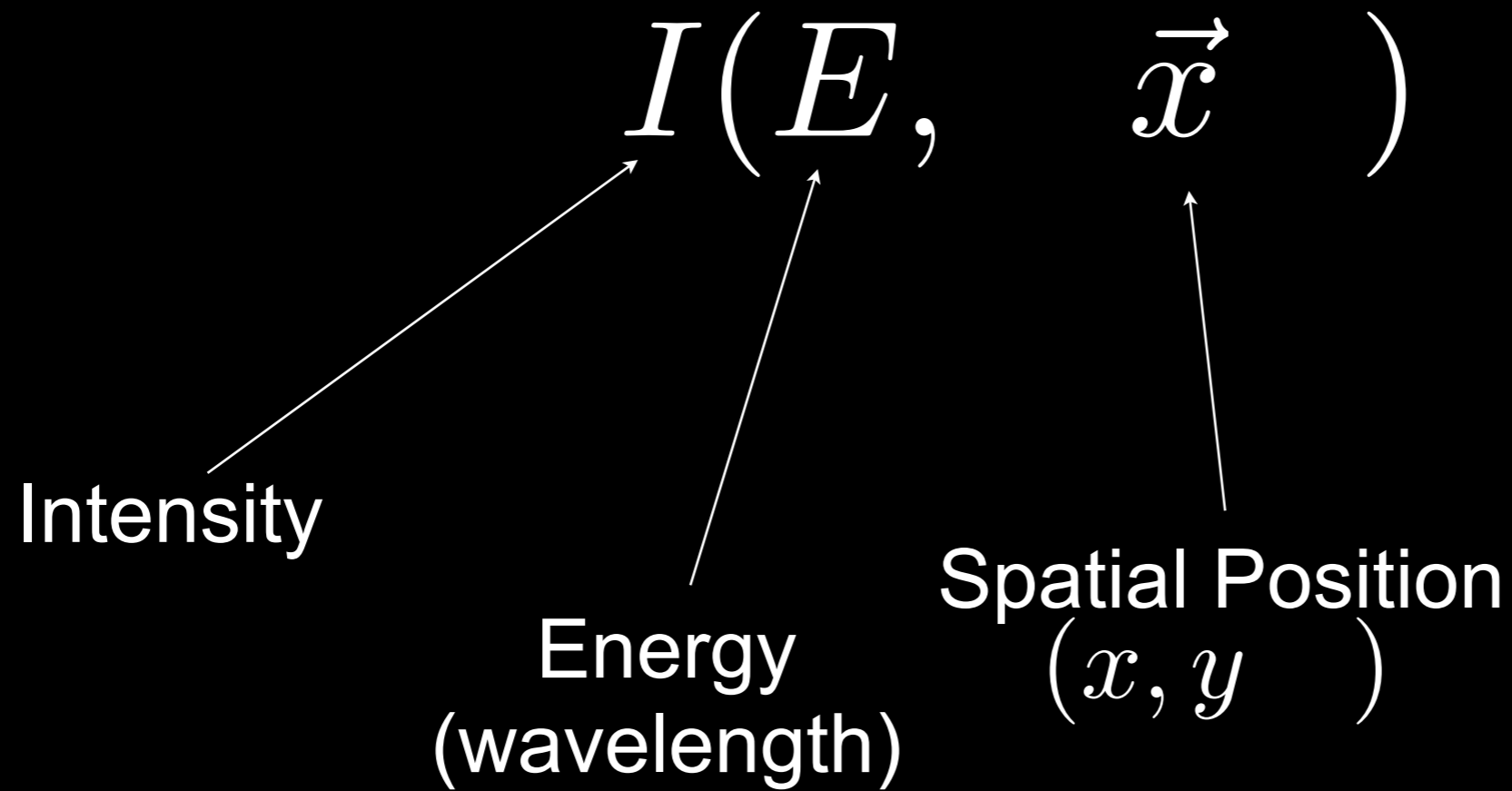
Time

Spatial Position
(x, y, z)



Cardiac Motion

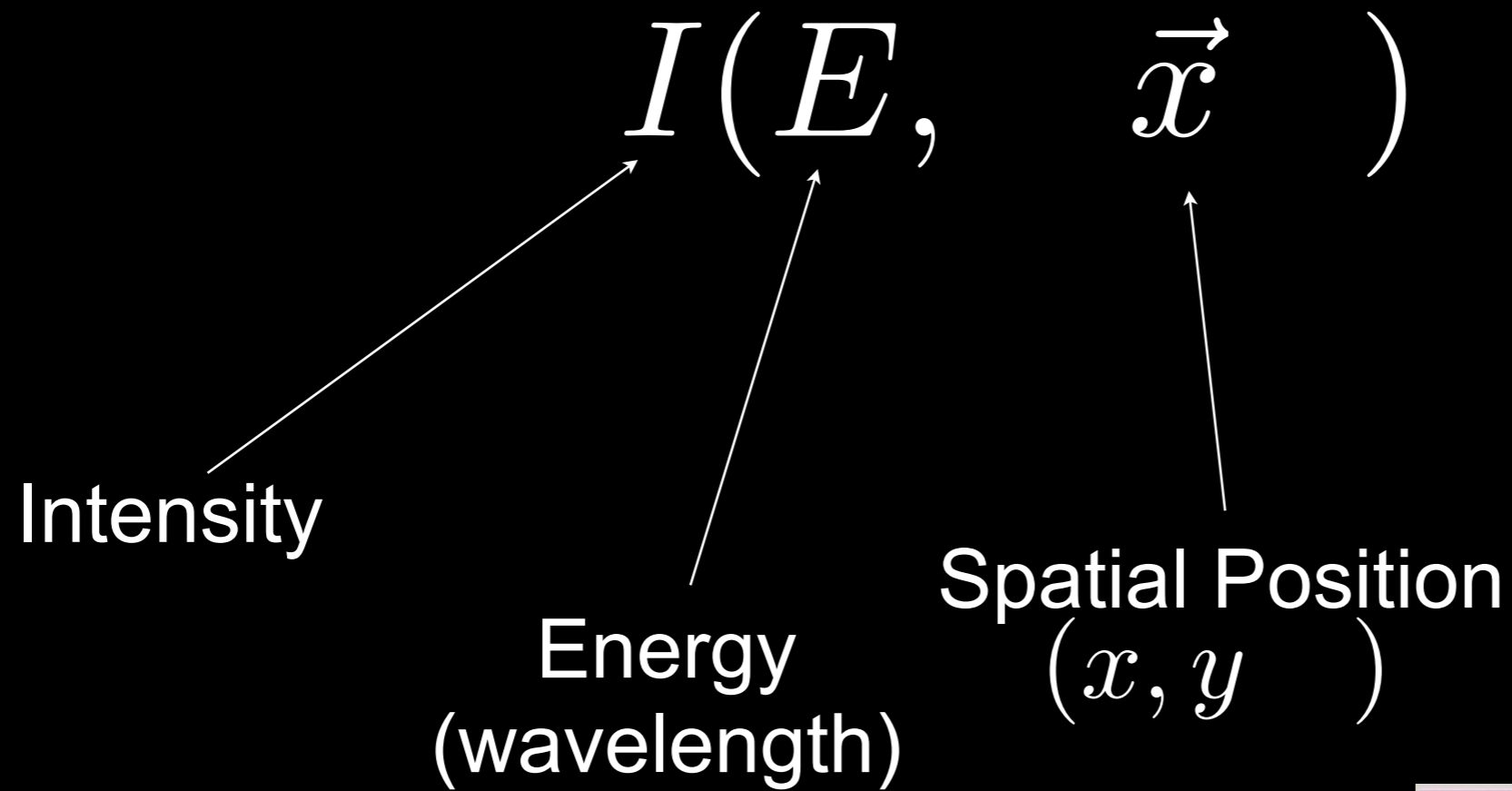
What can we observe?



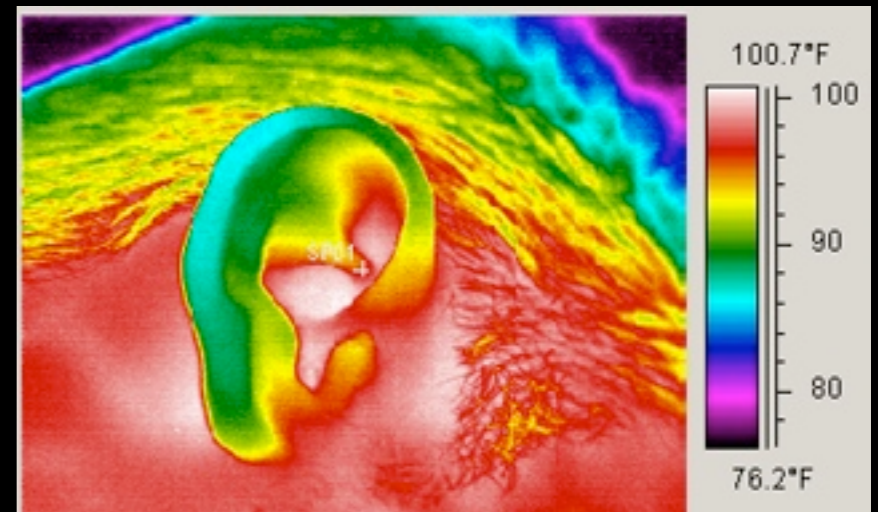
Optical (B,V,R) image
of NGC1333



What can we observe?



Human Ear,
Thermal Infrared



What can we observe?

$$I(s, \vec{x})$$

Intensity

Spatial Position
(x, y)

“State”
(e.g. polarization)

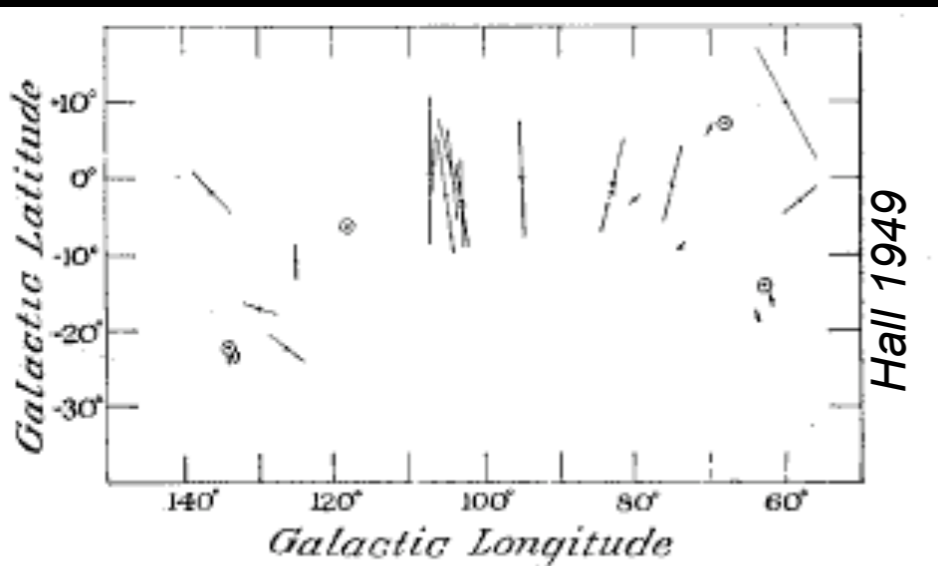


FIG. 4. Observational evidence that there is no one preferential orientation of the plane of polarization. Stars showing no polarization are represented by circles.

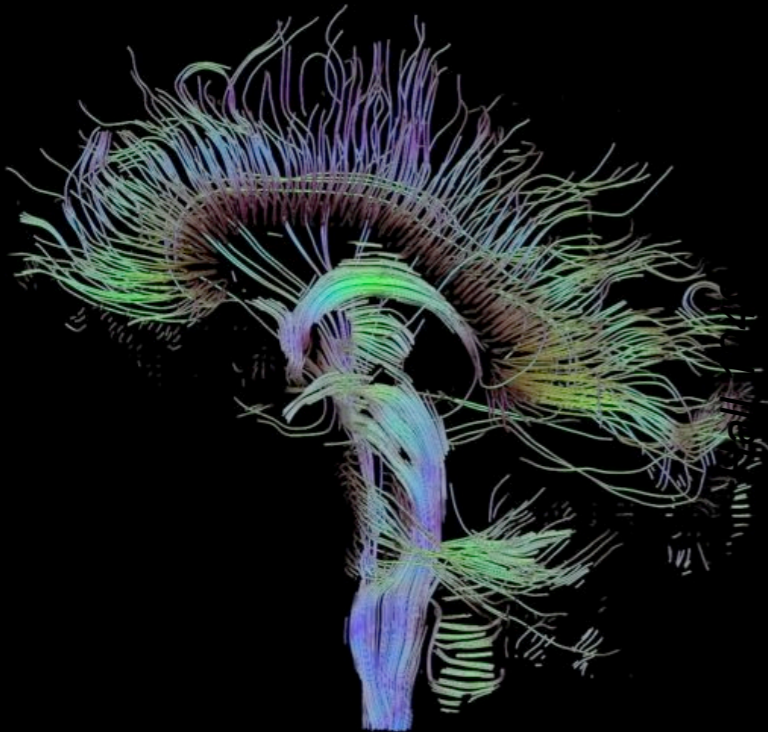
What can we observe?

$$I(s, \vec{x})$$

Intensity




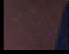

Spatial Position
(x, y, z)

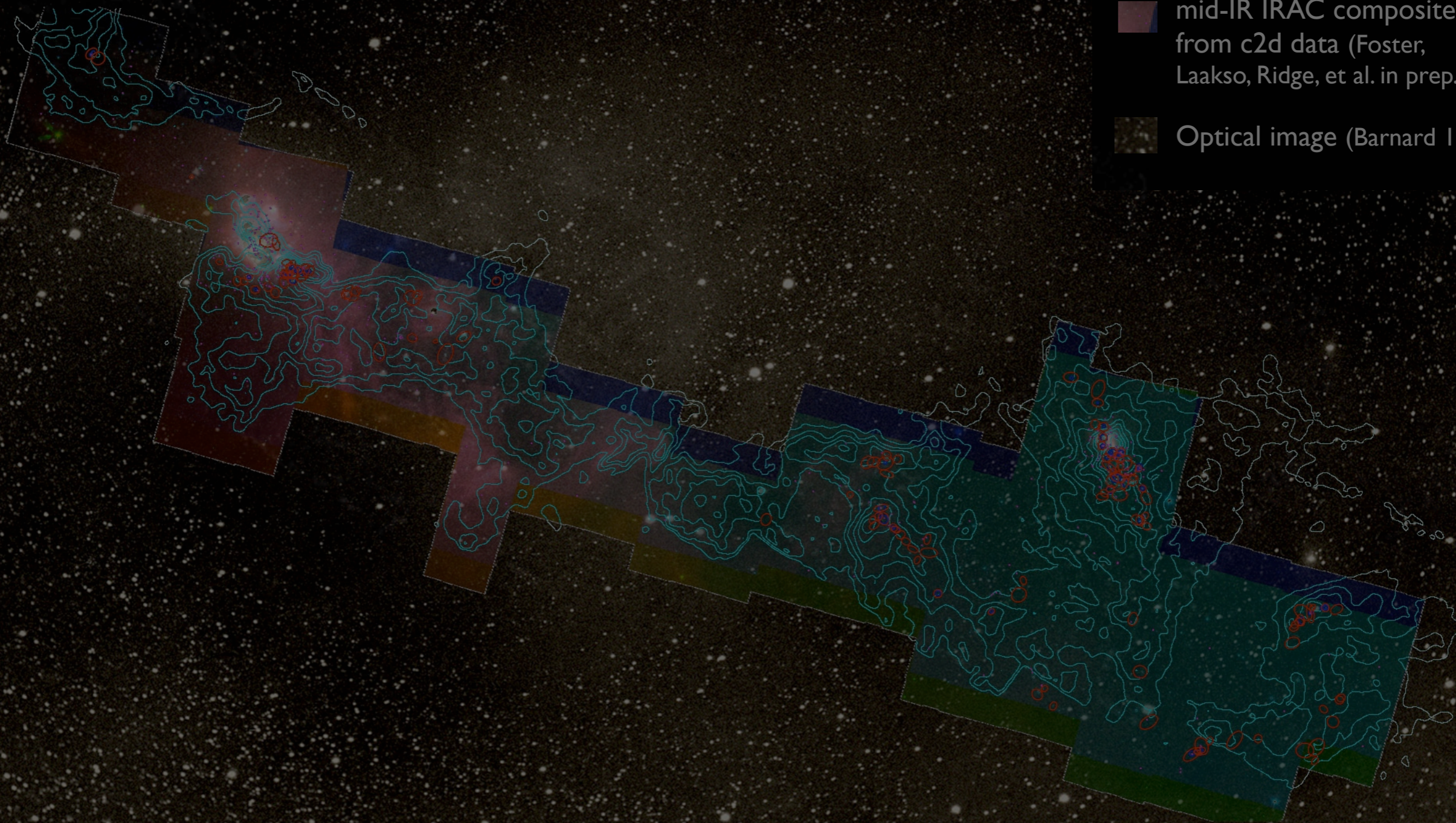
“State”
(~diffusivity)



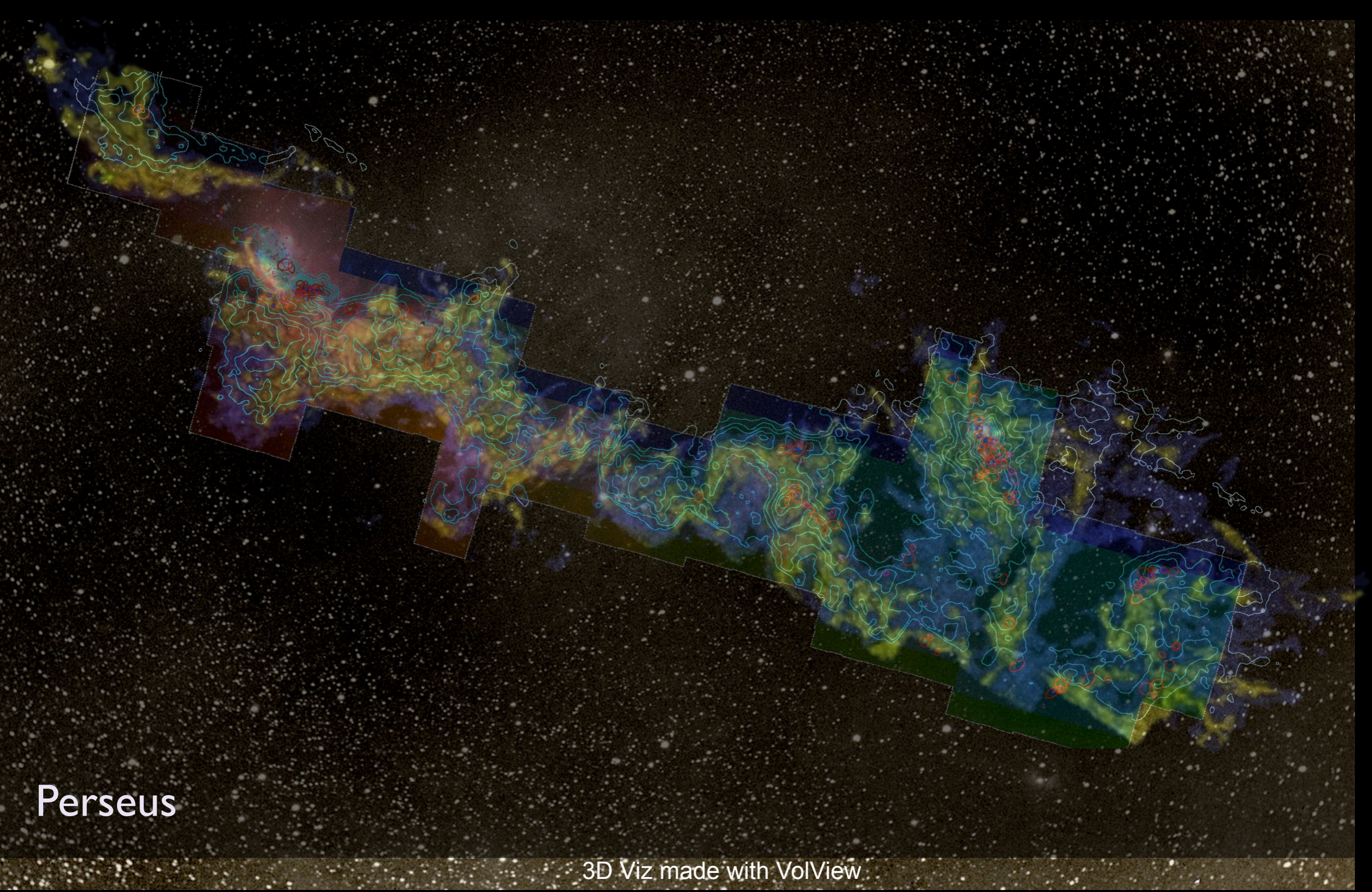
COMPLETE Perseus

image size: 1305 x 733
WL: 63 WW: 127

-  mm peak (Enoch et al. 2006)
-  sub-mm peak (Hatchell et al. 2005, Kirk et al. 2006)
-  ^{13}CO (Ridge et al. 2006)
-  mid-IR IRAC composite from c2d data (Foster, Laakso, Ridge, et al. in prep.)
-  Optical image (Barnard 1927)



m: 17249
Zoom: 227% Angle: 0



Perseus

3D Viz made with VolView

AstronomicalMedicine@iig

COMPLETE

Real 3D space



3D rendering: [GE Healthcare](#)

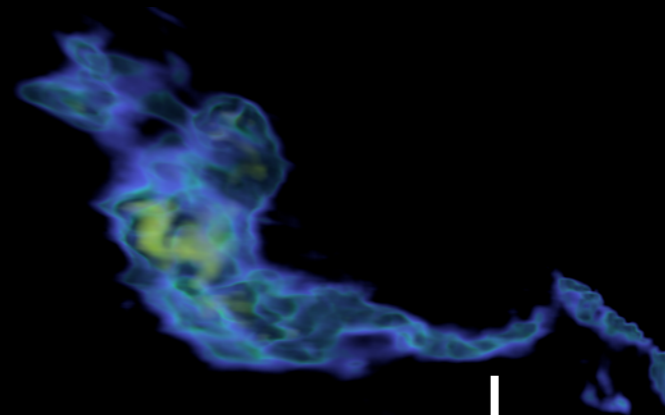
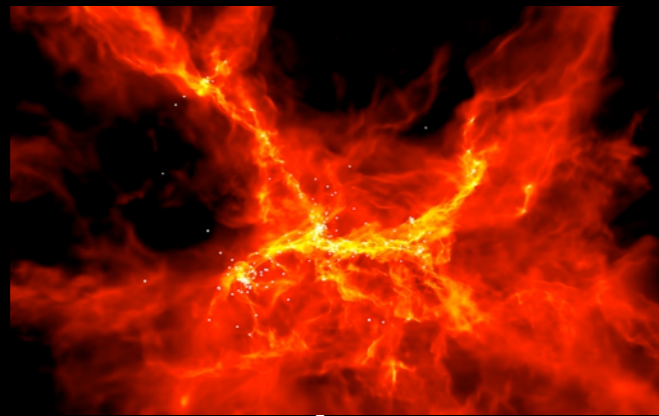
“Position-Position-Velocity” Space



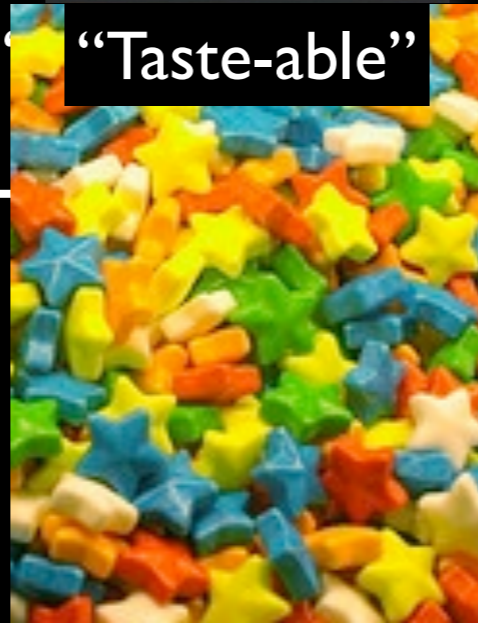
3D rendering: AstroMed / N. Holliman (U. Durham), using VolView (ITK-based)

simulations

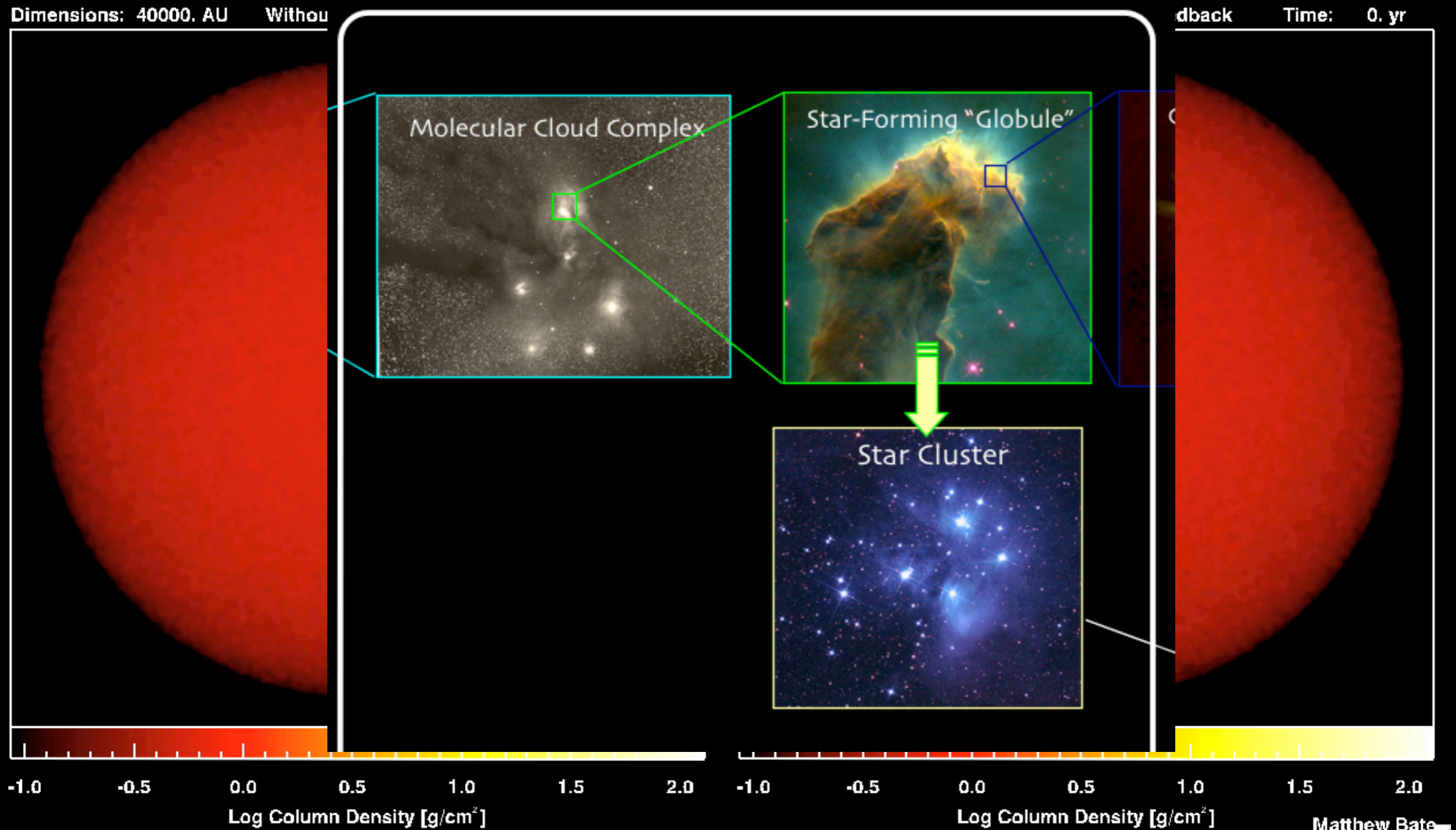
>2D
observations



“Taste-able”



“Tasting” Magnetohydrodynamic Simulations



Simulations of Bate 2009

Star Formation Taste Tests > Overview

https://iic.grouphub.com/projects/700257/project/log

taste test goodman alyssa

Back to Dashboard | Switch to a different project

Project Settings | My info | Log-out HELP


Star Formation Taste Tests CFA

Overview Messages To-Do Milestones Writeboards Chat Time Files

People & Permissions Search

Project overview & activity [New message](#) [New to-do list](#) [New milestone](#) [New file](#)

Welcome to the Tasting Room



This is the collaborative space for those who do simulations of star forming regions, and those who observe them. It was inspired, in the Fall of 2006, by the NSF proposal entitled "Star Formation Taste Tests," by A. Goodman & E. Rosolowsky. Today, it is used to host conversations about and short descriptions of simulatons, along with links to longer descriptions (e.g. Journal articles & web sites). In the future, we are planning to connect more enhanced descriptions of those simulations directly to online code bases and sample outputs, via the new [CADAC](#) site. So, stay tuned.

MONDAY, 13 APRIL 2009

Message [Relevant References relating to Bayesian Methods](#) Posted by Rahul S.

TUESDAY, 7 APRIL 2009

File [dustfit_slides.pdf](#) Uploaded by Rahul S.

WEDNESDAY, 18 FEBRUARY 2009

Writeboard [Taste Tests we Plan \(COMPLETE Group\)](#) Updated by Alyssa G.

To-do ~~Compare PPP and PPV dendrograms to determine the correct "paradigm" for mapping between the two. (Dendrograms and Simulations)~~ Completed by Alyssa G.

To-do ~~Taste Testing delivery to CADAC prior to Ringberg Meeting (Dendrograms and Simulations)~~ Completed by Alyssa G.

To-do ~~link to http://www1.astrophysik.uni-kiel.de/asd/ (Dendrograms and Simulations)~~ Assigned to Sarah B.

Writeboard [Re: Heitsch et al: Colliding Flows](#) Comment by Alyssa G.


WEDNESDAY, 21 JANUARY 2009

Message [Decadal Survey](#) Posted by Alyssa G.

THURSDAY, 20 NOVEMBER 2008

Comment [Re: "Toward a Prescriptive Understanding of Kennicutt-Schmidt Relations"](#) Posted by Alex L.

Comment [Re: "Toward a Prescriptive Understanding of Kennicutt-Schmidt Relations"](#) Posted by Alex L.



This project's RSS feed

[Subscribe to your project RSS feed](#) and be notified when someone posts a message, comment or file, or adds or completes a to-do item or milestone in this project. [What's RSS?](#)

People on this project

HCO

Alyssa Goodman
You are logged in right now

Sarah Block
Latest activity 25 days ago

Rahul Shetty
Latest activity 28 days ago

August Muench
Latest activity 28 days ago

Douglas Alan
Latest activity 28 days ago

Jens Kauffmann
Hasn't logged in recently

Michelle Borkin
Hasn't logged in recently

Michael Halle
Hasn't logged in recently

Felice Frankel
Hasn't logged in recently

Tim Kaxiras
Hasn't logged in recently

Tim Clark
Hasn't logged in recently

American Museum of Natural History

Mordecai-Mark Mac Low
Hasn't logged in recently

Héctor Arce
Hasn't logged in recently

Cal State Stanislaus

Christopher De Vries
Hasn't logged in recently

Calar Alto/MPI

Joao Alves
Hasn't logged in recently

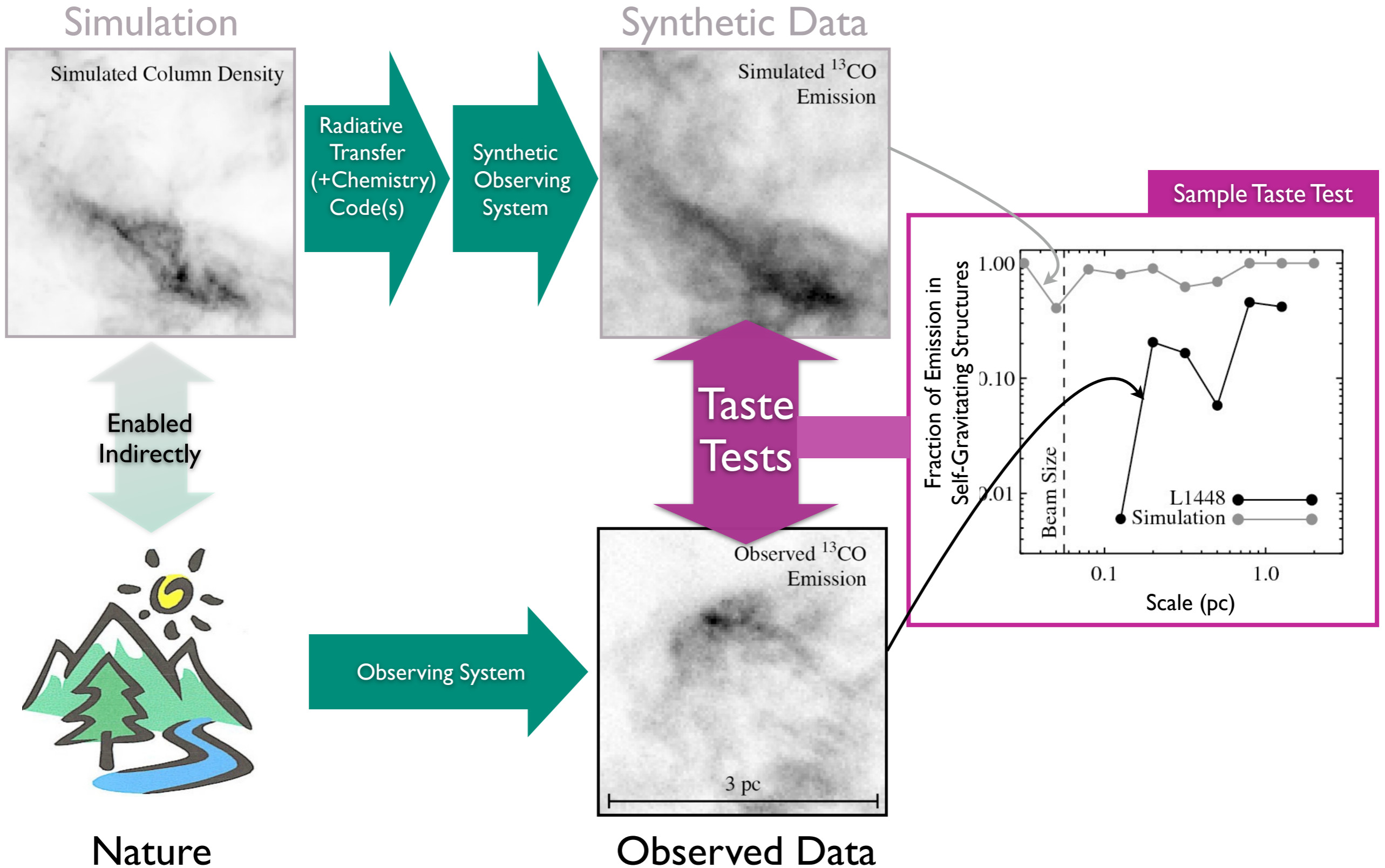
Caltech

Scott Schnee
Hasn't logged in recently

Tasting

$$I(E, s, \vec{x}, t)$$


The Taste-Testing Process



“Seeing” and “Tasting”

The Role Self-Gravity in Star Formation

LETTERS

NATURE | Vol 457 | 1 January 2009

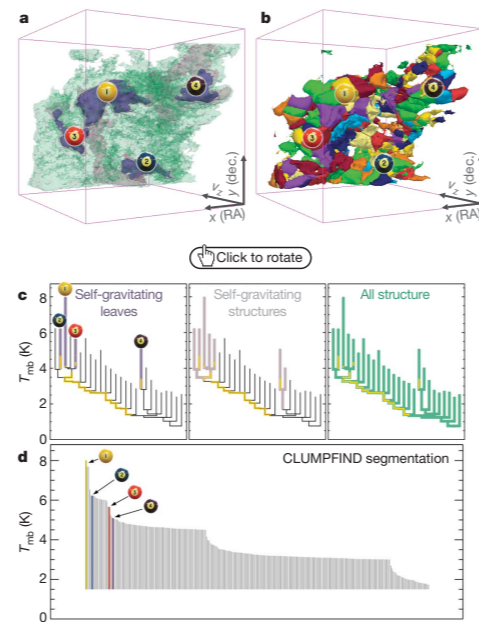


Figure 2 | Comparison of the ‘dendrogram’ and ‘CLUMPFIND’ feature-identification algorithms as applied to ^{13}CO emission from the L1448 region of Perseus. **a**, 3D visualization of the surfaces indicated by colours in the dendrogram shown in **c**. Purple illustrates the smallest scale self-gravitating structures in the region corresponding to the leaves of the dendrogram; pink shows the smallest surfaces that contain distinct self-gravitating leaves within them; and green corresponds to the surface in the data cube containing all the significant emission. Dendrogram branches corresponding to self-gravitating objects have been highlighted in yellow over the range of T_{mb} (main-beam temperature) test-level values for which the virial parameter is less than 2. The x - y locations of the four ‘self-gravitating’ leaves labelled with billiard balls are the same as those shown in Fig. 1. The 3D visualizations show position–position–velocity (p - p - v) space. RA, right ascension; dec., declination. For comparison with the ability of dendrograms (**c**) to track hierarchical structure, **d** shows a pseudo-dendrogram of the CLUMPFIND segmentation (**b**), with the same four labels used in Fig. 1 and in **a**. As ‘clumps’ are not allowed to belong to larger structures, each pseudo-branch in **d** is simply a series of lines connecting the maximum emission value in each clump to the threshold value. A very large number of clumps appears in **b** because of the sensitivity of CLUMPFIND to noise and small-scale structure in the data. In the online PDF version, the 3D cubes (**a** and **b**) can be rotated to any orientation, and surfaces can be turned on and off (interaction requires Adobe Acrobat version 7.0.8 or higher). In the printed version, the front face of each 3D cube (the ‘home’ view in the interactive online version) corresponds exactly to the patch of sky shown in Fig. 1, and velocity with respect to the Local Standard of Rest increases from front (-0.5 km s^{-1}) to back (8 km s^{-1}).

data, CLUMPFIND typically finds features on a limited range of scales, above but close to the physical resolution of the data, and its results can be overly dependent on input parameters. By tuning CLUMPFIND’s two free parameters, the same molecular-line data set⁸ can be used to show either that the frequency distribution of clump mass is the same as the initial mass function of stars or that it follows the much shallower mass function associated with large-scale molecular clouds (Supplementary Fig. 1).

Four years before the advent of CLUMPFIND, ‘structure trees’⁹ were proposed as a way to characterize clouds’ hierarchical structure

using 2D maps of column density. With this early 2D work as inspiration, we have developed a structure-identification algorithm that abstracts the hierarchical structure of a 3D (p - p - v) data cube into an easily visualized representation called a ‘dendrogram’¹⁰. Although well developed in other data-intensive fields^{11,12}, it is curious that the application of tree methodologies so far in astrophysics has been rare, and almost exclusively within the area of galaxy evolution, where ‘merger trees’ are being used with increasing frequency¹³.

Figure 3 and its legend explain the construction of dendrograms schematically. The dendrogram quantifies how and where local maxima of emission merge with each other, and its implementation is explained in Supplementary Methods. Critically, the dendrogram is determined almost entirely by the data itself, and it has negligible sensitivity to algorithm parameters. To make graphical presentation possible on paper and 2D screens, we ‘flatten’ the dendrograms of 3D data (see Fig. 3 and its legend), by sorting their ‘branches’ to not cross, which eliminates dimensional information on the x axis while preserving all information about connectivity and hierarchy. Numbered ‘billiard ball’ labels in the figures let the reader match features between a 2D map (Fig. 1), an interactive 3D map (Fig. 2a online) and a sorted dendrogram (Fig. 2c).

A dendrogram of a spectral-line data cube allows for the estimation of key physical properties associated with volumes bounded by isosurfaces, such as radius (R), velocity dispersion (σ_v) and luminosity (L). The volumes can have any shape, and in other work¹⁴ we focus on the significance of the especially elongated features seen in L1448 (Fig. 2a). The luminosity is an approximate proxy for mass, such that $M_{\text{lum}} = X_{13\text{CO}} L_{13\text{CO}}$, where $X_{13\text{CO}} = 8.0 \times 10^{20} \text{ cm}^2 \text{ K}^{-1} \text{ s}$ (ref. 15; see Supplementary Methods and Supplementary Fig. 2). The derived values for size, mass and velocity dispersion can then be used to estimate the role of self-gravity at each point in the hierarchy, via calculation of an ‘observed’ virial parameter, $\alpha_{\text{obs}} = 5\sigma_v^2 R / GM_{\text{lum}}$. In principle, extended portions of the tree (Fig. 2, yellow highlighting) where $\alpha_{\text{obs}} < 2$ (where gravitational energy is comparable to or larger than kinetic energy) correspond to regions of p - p - v space where self-gravity is significant. As α_{obs} only represents the ratio of kinetic energy to gravitational energy at one point in time, and does not explicitly capture external over-pressure and/or magnetic fields¹⁶, its measured value should only be used as a guide to the longevity (boundedness) of any particular feature.

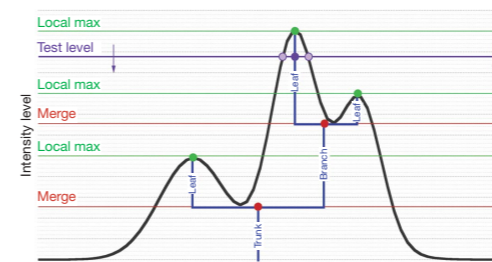


Figure 3 | Schematic illustration of the dendrogram process. Shown is the construction of a dendrogram from a hypothetical one-dimensional emission profile (black). The dendrogram (blue) can be constructed by ‘dropping’ a test constant emission level (purple) from above in tiny steps (exaggerated in size here, light lines) until all the local maxima and mergers are found, and connected as shown. The intersection of a test level with the emission is a set of points (for example the light purple dots) in one dimension, a planar curve in two dimensions, and an isosurface in three dimensions. The dendrogram of 3D data shown in Fig. 2c is the direct analogue of the tree shown here, only constructed from ‘isosurface’ rather than ‘point’ intersections. It has been sorted and flattened for representation on a flat page, as fully representing dendrograms for 3D data cubes would require four dimensions.

64

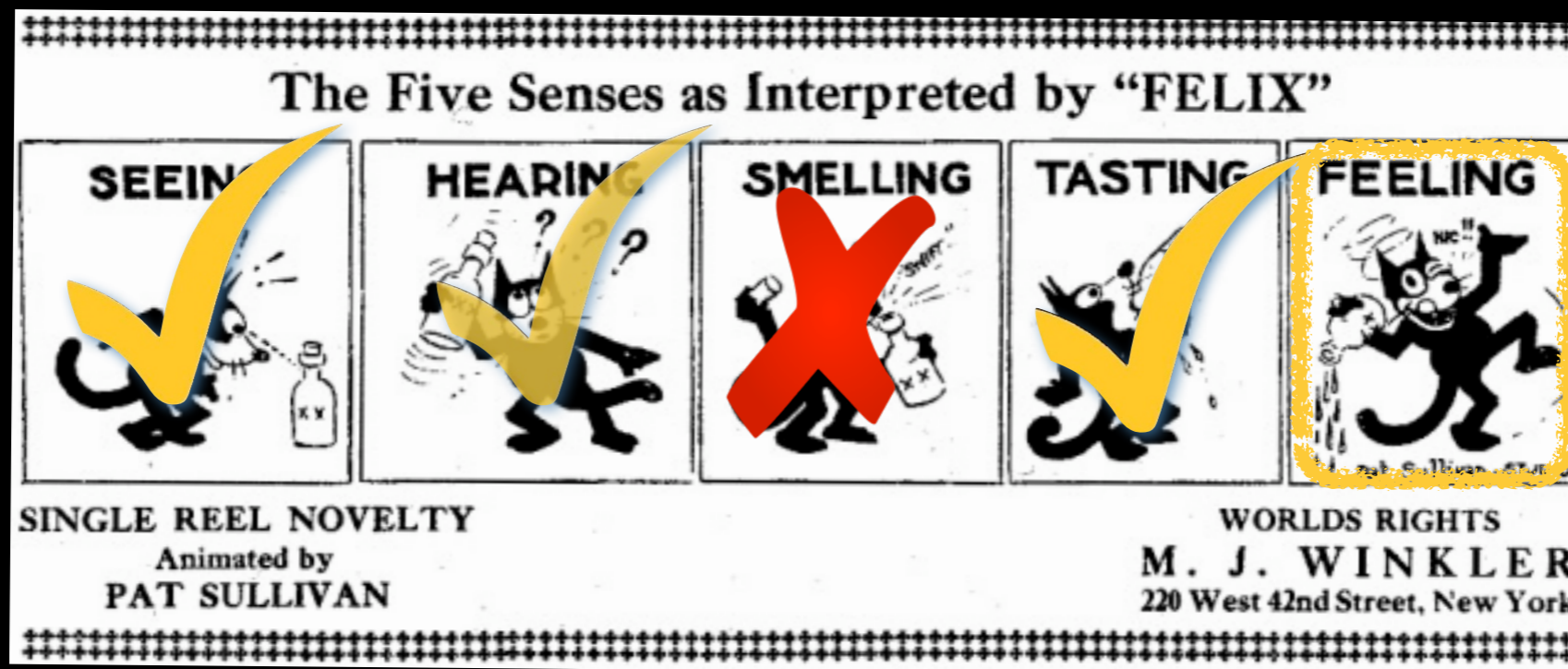
©2009 Macmillan Publishers Limited. All rights reserved



Goodman et al. *Nature*, 2009



Bonus: Using Extra Senses & Re-Using Software



Astronomy as I Touch it?

home
about the iic
research
education
people
events
employment
reaching the iic

INITIATIVE IN INNOVATIVE COMPUTING (IIC) NEWSLETTER
Stay informed on our latest news!
E-mail: *

 Subscribe
 Unsubscribe

Previous issues

IIC Member login

IIC

Initiative in Innovative Computing at Harvard

home > research


scientists' discovery room lab (sdr lab)

Lead investigators
Chia Shen (IIC) and Hanspeter Pfister (SEAS/IIC)

Project staff
Michael Horn, Meekal Bajaj, Matthew Tobiasz and Matthias Lee

Description

The Scientists' Discovery Room (SDR) is a next-generation visual digital laboratory for science discovery, collaborative learning and education. Our research focuses on experimenting with new modalities of human-computer interaction and visualization, to create a new genre of navigation, exploration and detailed analyses in multi-dimensional information spaces. All projects in SDR are in close collaboration with domain scientists and educators.



INVOLV is a generalizable multi-user interactive visualization framework for large hierarchical data sets. In this project, we address the visual layout of both the primary data representation and the overlay of alternate structures of the same data. Our first case study is the visualization of life on earth based on the Encyclopedia of Life (www.eol.org) and Tree of Life (www.tolweb.org). The user interface provides free-form exploration of more than 1.2 million named species while communicating issues of biodiversity and phylogeny. The current visualization combines a Voronoi Treemap tessellation with innovative human-computer interaction designs to support collaborative exploration and learning. Please visit www.involvweb.org for more information on this project.

CThru, a collaborative endeavor with Molecular and Cellular Biology faculty, aims to develop a self-guided learning environment. In CThru, we examine methods for constructing interactive video-based educational modules. Using the animation "The Inner Life of the Cell" as a testbed, CThru addresses research issues of embedding interactive visible objects, extensive multimedia information and manipulatable 3D models within a video flow, replacing sequential video viewing with the experience of exploring and manipulating in a multi-dimensional information space.

WeSpace is a collaborative work space that integrates a large data wall with a multi-user multi-touch table. WeSpace has been developed for a population of scientists who frequently meet in small groups for data exploration and visualization. It provides a low overhead walk-up and share environment for users with their own personal applications and laptops.

LivOlay is an interactive image overlay tool that enables the rapid visual overlay of live data rendered in different applications. Our tool addresses datasets in which visual registration of the information is necessary in order to allow for thorough understanding and visual analysis.

Slideshow: Tabletop Computers *Continued* By Meredith Ringel Morris

First Published December 2008

[Email](#) [Print](#) [Comments \(1\)](#) [Reprints](#) [Newsletters](#)

[Del.icio.us](#) [Digg](#) [Slashdot](#)

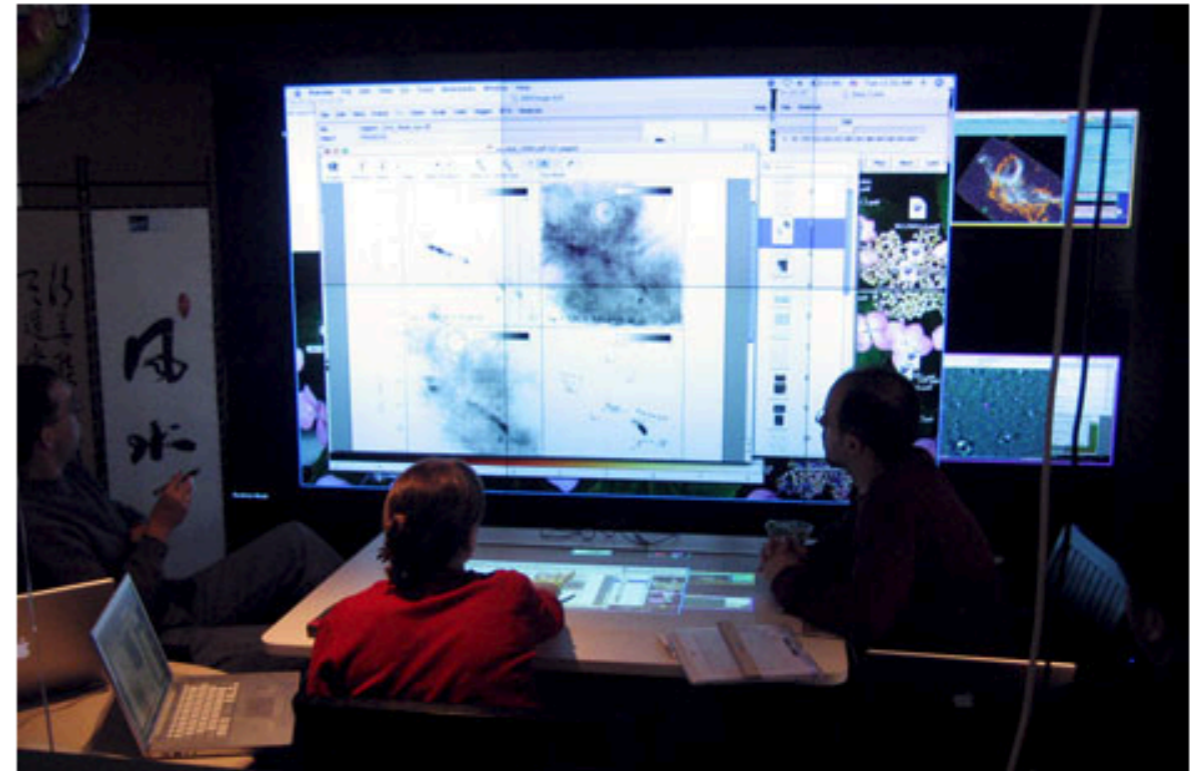


PHOTO: HAO JIANG, DANIEL WIGDOR, CLIFTON FORLINES, AND CHIA SHEN

UBITABLE: Users can interact with surface computers through auxiliary devices, such as laptops, phones, and PDAs. The display on the auxiliary device can convey private or sensitive content to a single user, while group-appropriate content can appear on the tabletop display. Chia Shen and her colleagues at Mitsubishi Electric Research Laboratories, in Cambridge, Mass., have explored auxiliary interactions with surface computers in their UbiTable project, in which two people with laptops collaborate over a tabletop display. Recently, Shen expanded the UbiTable into an interactive room called the WeSpace. People can share data on their laptops with other people in the room, using both a table and a large display wall. Here, three Harvard University astrophysicists discuss radio and IR spectrum images using the WeSpace.

The Scientists' Discovery Room (Shen & Pfister)



movie courtesy Daniel Wigdor, equipment now in Chia Shen's SDR lab at SEAS



What about data visualization...

...is easier now than before?

fast computation, animation, 3D

...was easier before than now?

craftsmanship

...should be easier in the future?

modular craftsmanship



Spitzer Space Telescope

• Jet Propulsion Laboratory
• California Institute of Technology
• Vision for Space Exploration

[Home](#)
[Images](#)
[Newsroom](#)
[Podcasts](#)
[Features](#)
[About Spitzer](#)
[Search / Site Info](#)

NEWSROOM

Press Releases

- Chronological
- By Subject
- Outside Institutions

What's Happening Archive

Visuals

- Image Use Policy

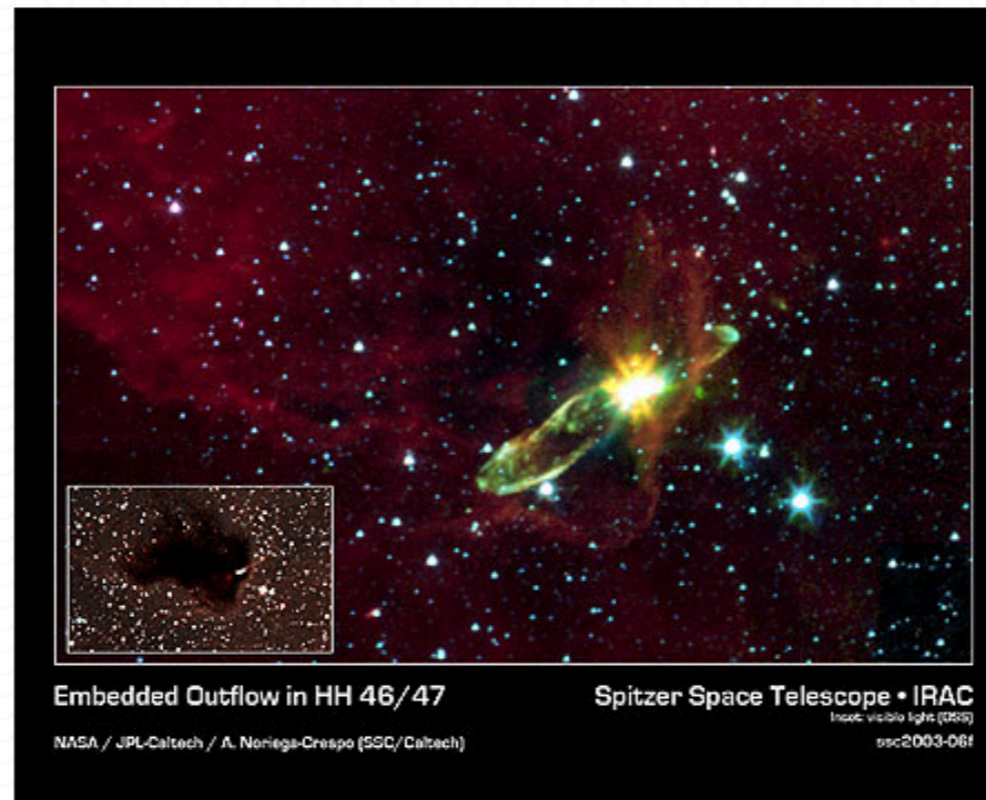
Update Notifications

- Mailing List
- RSS Feed (XML)

References

- Fast Facts
- Press Kit (.pdf)
- Fact Sheet (.pdf)
- Field Guides
- Glossary

Media Contacts



Embedded Outflow in HH 46/47

Spitzer Space Telescope • IRAC

NASA / JPL-Caltech / A. Noriega-Crespo (SSC/Caltech)

Inset: visible light (DSS)
ssc2003-06f

Credit: NASA/JPL-Caltech/A. Noriega-Crespo (SSC/Caltech), Digital Sky Survey

HH46/47

This image from NASA's Spitzer Space Telescope transforms a dark cloud into a silky translucent veil, revealing the molecular outflow from an otherwise hidden newborn star. Using near-infrared light, Spitzer pierces through the dark cloud to detect the embedded outflow in an object called HH 46/47. Herbig-Haro (HH) objects are bright, nebulous regions of gas and dust that are usually buried within dark clouds. They are formed when supersonic gas ejected from a forming protostar, or embryonic star, interacts with the surrounding interstellar medium. These young stars are often detected only in the infrared.

The Spitzer image was obtained with the infrared array camera. Emission at 3.6 microns is shown as blue, emission from 4.5 and 5.8 microns has been combined as green, and 8.0 micron emission is depicted as red.

HH 46/47 is a striking example of a low-mass protostar ejecting a jet and creating a bipolar, or two-sided, outflow. The central

HH4647

Share This

- ADD NOTE
- SEND TO GROUP
- ADD TO SET
- BLOG THIS
- ALL SIZES
- ORDER PRINTS
- ROTATE
- EDIT PHOTO
- DELETE



Embedded Outflow in HH 46/47 **Spitzer Space Telescope • IRAC**
Inset: visible light (0209)
 NASA / JPL-Caltech / A. Noriega-Crespo (SSC/Caltech) ssc2003-06f

Uploaded on January 6, 2009 by [Alyssa Goodman](#)

Alyssa_Goodman's photostream

16 uploads

browse

This photo also belongs to:

+ [astrometry \(Pool\)](#) x

Tags

- [Astrometrydotnet:version=10146](#) x
- [Astrometrydotnet:id=alpha-200901-20629873](#) x
- [Astrometrydotnet:status=solved](#) x

[Add a tag](#)

Additional Information

- All rights reserved ([edit](#))
- Anyone can see this photo ([edit](#))
- [Add to your map](#)
- Taken on [December 12, 2003](#) ([edit](#))
- [Photo stats](#)
- Viewed 7 times (Not including you)
- [Edit title, description, and tags](#)

[Flag your photo](#)

What...

I think we can aim for general, interoperable, (viz) tools with a “modular craftsmanship” approach.

...was easier before than now?



...should be easier in the future?

modular craftsmanship

Astronomy as I See, Touch, Taste, and Hear It

